COMPREHENSIVE ANALYSIS OF SWEEP ASSISTED ENHANCED ADAPTIVE FUZZY – P&O ALGORITHM FOR EFFICIENT MPPT PV SYSTEM

By

Muhammad Istianatur Rahman

13361005

A Thesis submitted to the Department of Electrical and Electronic Engineering (EEE) in partial fulfillment of the requirements for the degree of Master of Science in Electrical and Electronic Engineering

Department of Electrical and Electronic Engineering
BRAC University
September 2025

Declaration

It is hereby declared that

1. The Thesis submitted is my own original work while completing degree at BRAC University.
2. The Thesis does not contain material previously published or written by a third party, except where this is appropriately cited through full and accurate referencing.
3. The Thesis does not contain material which has been accepted, or submitted, for any other degree or diploma at a university or other institution.
4. We have acknowledged all main sources of help.

Student's Full Name & Signature:

____

Muhammad Istianatur Rahman

Approval

The Thesis titled "Comprehensive Analysis of Sweep Assisted Enhanced Adaptive Fuzzy – P&O Algorithm for Efficient MPPT PV System" submitted by

MUHAMMAD ISTIANATUR RAHMAN (13361005)

of Fall, 2025 has been accepted as satisfactory in partial fulfillment of the requirement for the degree of Master of Science in Electrical and Electronic Engineering on 6th Jan 2026.

Examining Committee:

Supervisor
(Chair)

____
Dr. A. S. Nazmul Huda
Associate Professor
Department of Electrical and Electronic Engineering
Brac University, Bangladesh

External Examiner:
(Member)

Tofael Ahmed
____
Dr. Tofael Ahmed
Professor
Department of Electrical and Electronic Engineering
Chittagong University of Engineering and Technology, Bangladesh

Internal Examiner:
(Member)

____
Dr. Shameem Ahmed
Associate Professor
Department of Electrical and Electronic Engineering
Brac University, Bangladesh

Departmental Head:
(Ex-Officio)

____
Dr. Md. Mosaddequr Rahman
Professor and Chairperson
Department of Electrical and Electronic Engineering
Brac University, Bangladesh.

Ethics Statement

I hereby declare that this thesis, which was written and finished without a copy, satisfies the research requirements for earning a degree in "Comprehensive Analysis of Sweep Assisted Enhanced Adaptive Fuzzy – P&O Algorithm for Efficient MPPT PV System." All the information and data are the reflection of my work. Also, the systems and software coding used here are done by me. I sometimes have collected some information from other papers where it is properly cited. Nothing in this paper relates to any other project or paper. I have completed total work with my own effort, and this unique work is done by taking assistance from supervisor and university.

Abstract

This research work proposes an algorithm that contains a dual-mode controller which uses adaptive fuzzy-enhanced P&O for fine-tuning steady-state control and sweep-based exploration for precise initialization for PV system with better oscillation, improved convergence speed and good tracking efficiency. This algorithm operates in two modes. The first mode is the sweep mode which is used to bring the operating point into the area of the Maximum Power Point (MPP). In this mode the duty cycle (D) is perturbed with a fixed step size, which sweeps the operating point across the entire I-V curve. Simultaneously, an initial estimate of the MPP voltage (Vmpp,est) is calculated using an empirical formula that incorporates real-time measurements of average irradiance (Gavg) and temperature (T). A sweep counter is increased if the operating point is far from the estimated MPP. After a predefined number the algorithm transitions to the second mode. In this mode the system first calculates the changes in power and voltage using this value the FIS computes the adaptive step size and using that the duty cycle is generated for the PV system. A 100kW PV system is modeled in MATLAB/SIMULINK, using the proposed technique the convergence time is obtained 16.8ms the voltage oscillation is 0.7V and the tracking efficiency is 99.6%.

Dedication

This work is dedicated with deepest love and gratitude to my parents and wife and my beloved family members. My path has been built around your unconditional support, encouragement, and sacrifices. I appreciate your undying belief in me, your encouragement to strive for greater things, and your support with every emotional, material, and spiritual trial. Your belief in me has been my biggest source of courage and inspiration to keep pursuing my objective.

Acknowledgement

I would like to express sincere thanks to my thesis supervisor Dr. A. S. Nazmul Huda, Associate Professor, Dept of Electrical & Electronic Engineering (EEE), BRAC University, for his supervision to make successful completion of the thesis. I am grateful to BRAC University for providing me the necessary help for the successful completion of this thesis.

Table of Contents

List of Tables

List of Figures

Chapter 1

INTRODUCTION

1.1. Background

The conventional energy foundations have directed a considerable push for the extensive adoption of renewable energy resources due to growing global power demand, resource depletion and environmental concerns [1], [2], [3]. Renewable energy sources include wind, solar, tidal, and geothermal energy have therefore become viable and eco-friendly substitutes for conventional supplies. Among them, solar photovoltaic (PV) systems offer a viable way of collecting solar energy considering its ease of use, scalability, and low maintenance requires, and pollution-free operation.

Furthermore, because of its accessibility, simplicity in installation, and almost negligible maintenance requirements, photovoltaic (PV) is expected to become one of the most widely used renewable energy sources [2]. Solar energy can be converted into electrical power using PV power generation equipment. However, temperature and irradiance have an impact on PV power oscillations. Since PV modules have a low conversion efficiency, solar electricity is still more expensive than fossil fuels [2]. The extremely low solar cell conversion efficiency of PV systems is a significant disadvantage [5], [6]. The performance of solar cells usually ranges from 9% to 17%, based on the weather [7].

A crucial aspect of creating an efficient PV system involves developing an efficient control algorithm. It is commonly recognized that using maximum power point tracking (MPPT) algorithms is one of the primary ways to increase efficiency in PV systems [8]. Due to the best feasible power transmission capabilities between the solar panels and the load or grid, power electronic converters are essential components of photovoltaic systems. These converters adjust to variations in environmental factors like temperature and irradiance while controlling voltage and current levels [9]. Maximum Power Point Tracking (MPPT), one of the fundamental technologies used in PV systems, has implications for optimizing energy output. In order to produce the most amount of power possible under varying conditions, MPPT algorithms dynamically modify the PV system's operating point [10].

Different MPPT strategies have been developed, including advanced artificial intelligence-based systems to more traditional approaches like Perturb and Observe (P&O) and Incremental Conductance (INC) [11]. The effectiveness of these methods depends on their tracking accuracy, convergence speed, and adaptability to partial shading conditions. Research on integrating efficient MPPT algorithms with cutting-edge power converters is still essential as PV systems develop in order to enhance overall system performance [12].

In this study, an advanced MPPT algorithm is proposed in order to reduce the oscillation and improve the convergence speed as well as tracking efficiency compare to the conventional and advanced MPPT techniques. The proposed algorithm is a hybrid adaptive fuzzy logic based modified P&O algorithm which operates in two modes in first mode it scans the mppt region and in second mode the adaptive fuzzy MPO fine tunes around MPP.

1.2. Problem Statement and Motivation

Solar cells exhibit nonlinear I-V and P-V properties that change on temperature and applied radiation [13], [14]. Consequently, the solar cell may extract the greatest power at an exact location on the P-V curve called the maximum power point (MPP) [15]. Maximum power point tracking (MPPT) algorithms have been developed and integrated into PV control systems that operate at this MPP. The MPP of solar panels under various irradiance profiles may now be tracked using several kinds of MPPT algorithms. These techniques can be categorized into two groups: soft computing MPPT methods and conventional MPPT methods. Conventional MPPT methods are known for their simplicity of use and inexpensive implementation costs, including perturb and observe (P&O), fractional open-circuit voltage, fractional short-circuit current, and hill climbing tactics [16].

The primary drawbacks of fractional open-circuit voltage and fractional short-circuit current methods are their limited use in low power conditions and their limited tracking accuracy. Even though the Hill Climbing (HC), P&O, and Incremental Conductance (IC) techniques are frequently employed and perform effectively in circumstances with constant sunlight, they are ineffective in situations with quickly fluctuating sunlight and partial shade.

Significant steady-state oscillations and slow tracking speed are among the main drawbacks of traditional approaches. Soft computing methods involving fuzzy logic control, sliding mode control, artificial neural networks, and metaheuristic-based algorithms like particle swarm optimization and adaptive algorithms have been developed to get around these limitations [17], [18].

Despite its simplicity and ease of use, the Perturb and Observe (P&O) algorithm is a good illustration of these drawbacks. With regard to its fixed-step size methodology, tracking speed and steady-state oscillation are inherently traded off. Since the operating point constantly oscillates around the maximum power point (MPP), a large step size results in significant power losses even if it allows for quick tracking during rapid shifts in irradiance [2]. A small step size, on the other hand, reduces these steady-state oscillations but significantly slows down the tracking reaction to dynamic changes, which could lead to the algorithm missing the global MPP in cases when the weather varies quickly. These fundamental weaknesses illustrate how ineffective traditional approaches are in a dynamic, real-world setting.

Moreover, high-power PV systems, like the 100 kW system under consideration in this study, make the challenges harder. The power losses caused by steady-state oscillations are not insignificant at this scale; they immediately result in a large decline in total energy output and economical viability. Furthermore, difficult operating conditions, such as partial shade and noticeable temperature effects, are more likely to affect large PV arrays [3]. A traditional P&O method may easily become stuck in one of the several local power maxima that partial shading introduces on the P-V curve, making it impossible to determine the true global MPP. The PV characteristics are further impacted by the increasing heat generation in high-power systems, a point that many traditional algorithms fail to effectively account for.

These difficulties provide a strong incentive to create an MPPT algorithm that is more reliable, effective, and intelligent. The optimal method should be able to track the global MPP reliably in partial shade conditions, manage dynamic irradiance and temperature changes, and overcome the trade-off between speed and oscillation.

To solve these problems, this thesis suggests a brand-new Sweep-assisted Enhanced Adaptive Fuzzy P&O Algorithm. This study intends to offer a high-performance solution especially designed for large-scale, high-power PV systems by combining an adaptive fuzzy logic controller for precise, fine-tuned tracking with a rapid sweep approach for initial peak estimate.

1.3. Objectives

The thesis objectives are given as following:

- To design a hybrid MPPT algorithm that combines the speed of a sweep method with the precision of a fuzzy logic controller.
- To evaluate the performance of the proposed algorithm under various dynamic conditions.

1.4. Thesis Contributions

This thesis contributes significantly to the fields of maximum power point tracking and photovoltaic power conversion. Addressing the drawbacks of current algorithms and offering a reliable, high-performance solution for large-scale systems are the primary objectives of these contributions. The following are the main contributions of this work:

A Hybrid MPPT Algorithm: The "Sweep-assisted Enhanced Adaptive Fuzzy P&O" algorithm is proposed and validated in this study. The fundamental trade-off between tracking speed and steady-state oscillations that impacts traditional approaches is resolved by this hybrid approach. The algorithm achieves rapid convergence without compromising efficiency by introducing a fast initial sweep to estimate the MPP, followed by a precise fuzzy logic-based P&O controller. In addition to exhibiting resilience against becoming trapped in local maxima under partial shading conditions, this clever, adaptive control strategy is made to maintain high performance under a variety of dynamic environmental conditions, such as abrupt changes in temperature and irradiance.

A Detailed 100 kW PV Boost Converter Simulation Model: Using the Simulink, an accurate and dynamic simulation model of a 100 kW PV system is created. This model functions as a virtual test to assess the suggested MPPT algorithm's performance. It accurately depicts the dynamics of a high-power boost converter, the electrical properties of a sizable PV array, and the relationship between the control algorithm and the power stage. This comprehensive model offers a strong foundation for in-depth examination and validation of the theoretical ideas, an essential stage prior to any hardware deployment.

A Quantitative Performance Analysis: A comprehensive, data-driven performance analysis of the suggested algorithm is presented in this thesis. Important performance indicators are quantitatively assessed, such as tracking speed, steady-state power ripple, MPPT efficiency, and total system energy output. To illustrate the proposed algorithm's higher performance, its output is methodically compared with that of a traditional P&O algorithm. In order to present a comprehensive and convincing case for the effectiveness of the new control method, the analysis is carried out under both steady-state and dynamic operating situations, including partial shading scenarios.

1.5. Thesis Outline

This thesis is organized into five chapters, each building upon the previous one to provide a comprehensive analysis of the proposed MPPT algorithm.

Chapter 1: Introduction: This chapter discusses the importance of PV systems and the need for effective MPPT algorithms in order to set the groundwork for the research. It summarizes the thesis's main contributions, gives the main problem statement, and describes the study's goals.

Chapter 2: Literature Review: A detailed analysis of the current studies is given in this chapter. The basics of PV systems, how DC-DC boost converters work, and an in-depth review of both traditional and sophisticated MPPT algorithms—with an emphasis on fuzzy logic control and the Perturb and Observe methods are all covered.

Chapter 3: Methodology: The Proposed MPPT Algorithm: The technical aspects of the study are covered in this chapter. It provides an in-depth description of the new hybrid MPPT algorithm, the particulars of its implementation in the Simulink environment, and the mathematical models of the PV system and boost converter.

Chapter 4: Results and Discussion: The results of the simulation are shown and explained in this chapter. It offers a numerical evaluation of the suggested algorithm's performance in a range of steady-state and dynamic scenarios, highlighting the new method's outstanding results through comparisons with a traditional P&O algorithm.

Chapter 5: Conclusion and Future Work: This final chapter summarizes the key findings and contributions of the thesis. It concludes with recommendations for additional research, including possible hardware implementation and additional algorithmic improvements.

Chapter 2

Literature Review

2.1. Overview of Literature Review

This literature review founds the initial framework for the study by observing the history and essential restraints of photovoltaic (PV) energy, which produces a dire need for power optimization. It emphasizes Maximum Power Point Tracking (MPPT) as the key technological approach for optimizing PV system energy gathering. Both conventional and clever MPPT techniques are methodically categorized and reviewed in this chapter. The state of the art is summarized in this methodical analysis, which also highlights its advantages and disadvantages. As a result, the review pinpoints the performance gaps that spur the creation of the improved MPPT algorithm put forward in this thesis.

2.2. History of Photovoltaic Energy

Becquerel identified the photon-voltage relationship in 1839 while investigating how light affected electrolytic cells [19]. Adams and Day also observed the same behavior on solid selenium later, in 1877. Fritz proceeded ahead to design the first photovoltaic cell in 1883, albeit it had a very low conversion efficiency of only 1%. The contemporary PV module, however, required a long time to design and was manufactured at Bell Laboratories in 1954 [20]. This module had a conversion efficiency of roughly 6–10% [21]. Due to its high cost, PV energy was only used in the military and aerospace sectors. Several PV module types, including thin-film and polycrystalline Si (pc-Si) semiconductors, were developed in the 1960s [22]. These types had a high manufacturing capacity, structural integration, and an improved efficiency of approximately 15%. This led to a decline in the capital installation cost for large-scale photovoltaic system generation. Investment in this energy source was stimulated by the oil crisis of the 1970s and the new PV system's characteristics [23].

As a result, a number of universities, including Delaware University have installed PV system. This PV module's conversion efficiency was 17% [20]. With a conversion efficiency of roughly

20%, the first large-scale PV plant of over MW constructed for industrial use occurred in the 1980s. However, the 1990s saw the production of the first PV system for residential use as a result of programs that recommended investing in PV resources. A PV cell's conversion efficiency had risen to 30% by this point [24]. Researchers created a new two-junction photovoltaic cell in 2000 that had a conversion efficiency of over 33%. With a conversion efficiency of over 42%, they improved this new PV cell based on multi-junctions ten years later. This multijunction PV cell was able to achieve a conversion efficiency of over 44% in 2012 thanks to the efforts of researchers at the National Renewable Energy Laboratory (NREL) [25], [26].

Monocrystalline, thin-film pc-silicon, thin-film amorphous, thin-film chalcogenide, and concentrated PV cells are among the several types of PV cells that have been developed recently [27]. Water pump systems, high-way signs, street lights, roadside emergency phones, surveillance cameras, standalone PV systems, and grid-connected PV systems are just a few of the many uses for them [28]. The primary historical advancements in PV technology with respect to conversion efficiency, according to several research initiatives [21–26], are shown in Fig. 2.1.

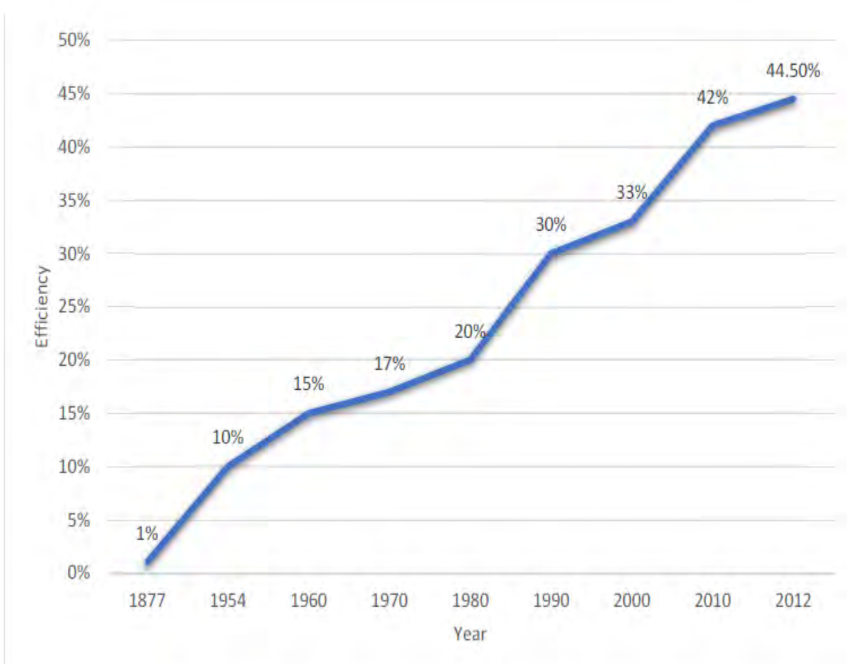

Fig. 2.1. The historical development of PV energy [21-26]

2.3. Photovoltaic Technology Constraints

2.3.1. Photovoltaic Cell Efficiency

Based on the local weather, a photovoltaic cell's output power varies [29], [30]. In essence, when irradiance rises, the PV array's generating power rises as well because high photon voltages strike the cell's electron-hole, increasing the PV output current. At high operating temperatures, on the other hand, this falls because the PV semiconductor's band gap widens and the open circuit voltage of the PV cell declines. During this stage, when input irradiation is captured, the mobility of PV electrons becomes less valent, which reduces energy loss.

2.3.2. PV generation stability

During designing a grid-connected PV system, the variation in PV output power due to moving clouds is seen as a significant problem [31] and [32]. The PV system's performance may be affected by a number of problems, including voltage oscillation and increase. In other words, very variable meteorological conditions can have a substantial influence on the stability and dependability of PV power output, particularly when it comes to large-scale PV generating. Controlling the energy flow all over a hybrid power system is crucial to adjusting the PV generation for the utility grid because this problem is unusual in conventional power systems.

2.3.3. PV load mismatch

The value of the load additionally determines how a PV array operates in terms of voltage [33], [34], and [35]. When the output power generation of a PV array is less or more than the power load, PV voltage operation will either reduce or increase to a new operating point. PV generation efficiency will consequently decrease. Additionally, the equipment of a grid-connected PV system may sustain damage if a large-scale PV plant disconnects as a result of an interruption.

2.3.4. How long a PV module lasts after installation

According to the majority of PV manufacturing companies, a PV module's lifespan is usually 20 years, and its production should be at least 80% of its rated power [36]. Nonetheless, a number of studies suggest an installed PV system's lifetime reduces by approximately 0.2% annually due to weather-related operational issues [37]. This is why abrupt changes in the weather lead to significant shifts in PV voltage.

2.4. Techniques for Maximum Power Point Tracking

An essential aspect of PV system design is the maximum power point tracking (MPPT) technique, which tracks a PV array's MPP and enhances the stability and reliability of the Photovoltaic system in the presence of a grid connection [38]–[40]. It also tackles the challenge of matching the PV load and the issue of partial shade situations. Therefore, it helps extend the life of a PV module that has been installed. In general, the primary concerns in working to develop an MPPT method for a PV system are tracking efficiency, cost, energy loss, and kind of implementation [42].

Given these, several well-liked MPPT methods have been put out for PV systems. These can be categorized into two categories: artificial intelligence (AI) techniques, such as the Fuzzy Logic Controller (FLC) [45], artificial neural network (ANN) [46], Adaptive Neuro-Fuzzy Inference System (ANFIS), and particle swarm optimization (PSO) [32], and conventional techniques, such as constant voltage (CV) [42], fraction open circuit voltage (FOCV), Perturb and Observe (P&O) [43], and incremental conductance (IC) [44].

Since it can calculate the MPP without the requirement of an input sensor, the CV technique is the most straightforward MPPT algorithm for a PV system [42]. According to Eq. (2.1), this method makes the assumption that variations in the PV panel, such as irradiance and weather temperature, are insignificant and that the constant reference voltage ($V_{ref.}$) is adequate to achieve performance around the MPP.

$$V_{ref} = k \times V_{OC} \tag{2.1}$$

where Voc is the open circuit voltage of a PV array and k is a constant between 0.71 and 0.78 that is adjusted depending on the characteristics and weather of an installed PV array. Thus, it is anticipated that the PV array's operating point will be around the MPP by regulating the PV voltage to match a predefined reference voltage. However, as this may vary from place to place, climatic installing data must be gathered in order to determine the fixed voltage reference. This technique's primary benefit is its rapidity in attaining the steady state situation, especially under diffused and low radiation settings [47].

It just computes the MPP roughly, though. FOCV control is an additional straightforward technique for the MPPT controller. This technique monitors the PV module's MPP by using a linear proportional relationship between the installed PV module's operating voltage at MPP and its open circuit voltage, which is determined using the datasheet of the installed PV module and is displayed in (2.1). Depending on the installed PV array's weather conditions, the constant (k) in (2.1) is continuously modified. Compared to the CV method, this approach finds the MPP more accurately in a variety of meteorological circumstances. It does, however, only compute the MPP roughly.

The MPP can be precisely calculated using the P&O-MPPT as it mentioned in Eq. (2.2) and Eq. (2.3). This algorithm's main function is to determine the PV power using the PV module's detected voltage and current information. Following a comparison with the prior power and voltage, the algorithm is used to modify the power converter's duty cycle appropriately. Its low cost and easy implementation make it a popular solution for PV-MPPT [48].

$$\frac{dP}{dV} > 0 \text{ left of MPP} \tag{2.2}$$

$$\frac{dP}{dV} < 0 \text{ right of MPP} \tag{2.3}$$

Designing an optimal MPPT controller requires knowledge of a PV system, which leads to erroneous fuzzy rules and FLC system membership functions. Numerous changes have been proposed for an adaptive and optimized defined membership function of the conventional FLC-MPPT employing a variety of optimization techniques in order to overcome those problems. For instance, as demonstrated in [51], a genetic algorithm, the PSO algorithm, or the M5P model tree. Although the drift issue with varying irradiance is avoided by these solutions, their hardware implementations become more intricate.

The standard FLCMPPT problem was recently resolved by employing an MPPT with ANN approach, which uses numerical quantification data to produce a heuristic output function and eliminates the need for a thorough understanding of the PV parameters in order to construct an optimal MPPT controller [50]. Therefore, when compared to FLC-MPPT, the ANN-MPPT approach has a higher tracking speed for transient states and less oscillation around the MPP point at steady state conditions. Furthermore, it is more accurate when handling the MPP under atmospheric conditions that are changing quickly. Consequently, its efficiency surpasses that of the traditional FLCMPPT approach.

Yet, the main drawbacks of the ANN system are its training approach, black box work, and delayed training. In order to overcome these constraints, a number of adjustments have been suggested to improve the ANN model's performance through a variety of optimization techniques, as seen in [46], [49]. These techniques' methods may be broken down into three categories: choosing the best training data, determining an ANN model's optimal topology, and figuring out the ANN algorithm's parameters. Nevertheless, this method has a large training error.

Since the ANFIS method is integrated into the ANN and FLC system, it offers the most effective intelligence technique for PV systems. Based on a fuzzy inference system, it is a modified neural network technique. Furthermore, the ANFIS-based MPPT approach responses faster, oscillates less, and is more accurate when dealing with the MPP for different weather conditions. When creating an effective ANFIS-MPPT controller, obtaining precise training data and fine-tuning the ANFIS model are major obstacles. Recent years have seen a number of approaches based on training data from experiments and theory.

2.5. Review for MPPT Methods

The challenging aspect of solar energy is its dynamic nature, which allows it to produce varying voltages and powers depending on the surrounding circumstances. These variables include things like wind speed, shade, and sun insolation angle. Consequently, not all electrical loads will generate the maximum amount of electricity [52], [53]. With the right controllers, MPPT approaches can maximize the power that can be extracted from PV setups. PV modules can be operated at maximum power using a variety of MPPT approaches. However, the efficiency of the specific method relies on its capacity to track rapidly shifting weather patterns. Therefore, these strategies are categorized based on the tracking nature under PSCs.All classified procedures are discussed [51], [54], and are grouped into the following categorization.

a) Classical PV MPPT.
b) Intelligent PV MPPT.
c) Optimization PV MPPT.
d) Hybrid PV MPPT.

Constant voltage (CV), incremental conductance (InC), open circuit voltage (OCV), short circuit current (SCC), hill climbing (HC), perturb and observe (P&O), enhanced P&O, adaptive reference voltage (ARV), ripple correlation control (RCC), and lookup table method are among the methods used for classical MPPT [54], [55]. Through their simpler algorithms, these methods are easy to construct. Under homogeneous irradiation conditions, the PV is most effective because it will only produce one GMPP. However, these algorithms oscillate around the MPP very quickly, which causes power loss. Above all, these traditional approaches that ignore the impact of partial shade situations fail to track the actual MPP. Fuzzy logic control (FLC), artificial neural networks (ANN), sliding mode control (SMC), Fibonacci series-based MPPT, and Gauss-Newton approach-based MPPT are examples of intelligent-based approaches [54], [56]. These methods are proposed to offer the maximum level of accuracy in dynamic weather circumstances. They have extremely high tracking speeds and efficiency. These approaches also suffer from large data processing for system training in advance and extremely sophisticated control circuits. One remarkable method that does not necessitate system expertise for MPPT implementation is FLC. Although ANN is a faster tracking method, its accuracy involves a massive amount of data. It stores temperature and dynamic irradiation as data sets and uses them as inputs. Although SMC is the most advanced technique, faster tracking speeds make implementation simpler. Two techniques, Fibonacci and Gauss-Newton, are developing more quickly because of their capability to track MPP intelligently by instantly altering the search range.

Cuckoo search-based, particle swarm optimization (PSO), gray wolf optimization (GWO), ant-colony optimization (ACO), and artificial bee colony (ABC) are examples of optimization-based methodologies [54], [57]. These techniques also have a tendency to look for actual MPP in dynamic environments. The PSO approach reduces steady-state oscillations and provides a faster tracking algorithm. Furthermore, low-cost microcontrollers make it simpler to execute these strategies. GWO can find the best way to work more quickly, much like a wolf that never stops looking for its prey. The most important evolutionary method that is independent of system information is this GWO. Cuckoo search-based MPPT is another bio-inspired algorithm that uses the levy flying methodology to achieve the optimal MPP point by utilizing the nature of brood parasitism. Two techniques that track GMPP without the need for temperature and radiation sensors are ACO and ABC, both of which make use of evolutionary processes.

Combining intelligent or optimum MPPTs with classical MPPTs is known as hybrid-based MPPT approaches [58]. The optimal fusion of intelligence and optimization is also included in some hybrid approaches. In these combined MPPTs, the tracking methodology is used in two stages: first, the MPP is estimated, and second, advanced methodologies are used to refine the MPP. First, the MPP on the P-V curve is determined using conventional or classical methods. The goal of this stage is to get the set-point as close to MPP as is practical. Second, the set-point is developed to attain the actual MPP utilizing advanced techniques. Several hybrid techniques, such as FPSO, ANFIS, GWO-P&O, PSO-P&O, and HC-ANFIS, are elaborated upon in this study.

2.5.1. Traditional MPPT Methods

2.5.1.1. MPPT Based on Constant Voltage (CV)

Although the technique is swift, simple, and easy to use, its accuracy is not very high. The regulating mechanism compares this PV voltage with a predetermined reference voltage equal to the VMPP in order to get the PV power to run close to the MPP. This CV approach is used for uniform irradiation settings and ignores the effects of temperature and insolation. This CV approach's projected MPP point differs slightly from the real MPP. With regard to this, the operational point is not synchronizing the MPP, and the optimal reference voltage needs to consider different topographical locations in order to lower the error value. The schematic block diagram for the CV MPPT approach is shown in Fig. 2.2.

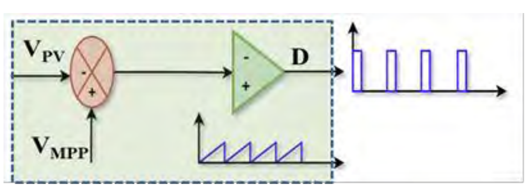

Fig. 2.2. The CV MPPT technique's schematic block diagram.

With this approach, only one sensor is needed, namely for voltage measurement to obtain the PV module voltage VPV and the correct D for the converter [59]. The Voc must be measured using this method at regular intervals. Furthermore, this method operates under conditions with minimal temperature change [60]–[62]. The innovative MPPT algorithm was successfully implemented by

H. Wang et al. [63] utilizing a CVCC (constant voltage constant current) DC-DC converter, allowing the researchers to precisely identify the optimal point.

2.5.1.2. MPPT based on Adaptive Reference Voltage (ARV)

Unlike the CV MPPT, the ARV approach takes climate factors into account. This system is a little more expensive than the conventional CV system since it uses two more sensors to estimate the T and G levels and one more sensor than the P&O approach. However, this cost element was offset by the gain in efficiency. Because it can function in a variety of weather conditions, the ARV-based MPPT system is an extension strategy to the constant voltage method. The reference voltage (RV) for MPPT is adjusted by the purposeful radiation and temperature levels. Fig. 3 shows the ARV MPPT method's schematic block model. A truth table is used to record the comparative RV when the functioning possibility of the radiation at a specific temperature is divided into many divisions. The corresponding proportional-integral (PI) controller is used to compensate for the error between the reference and assessed PV voltages in order to give an appropriate D proportionate to the fitted converter that is used.. The simulated comparison between this method and the CV methodology is provided by M. Lasheen et al. [64]. Both methods' efficiency under constant radiation settings (around 1000 W/m2) were nearly identical (> 99.7%). However, when irradiation drops to 400 W/m2, CV efficiency drops to 98.3%, while our ARV approach maintains the same efficiency under all varied radiation levels.

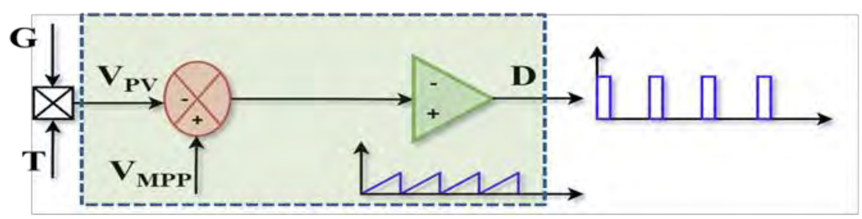

Fig. 2.3. ARV MPPT method schematic block diagram.

2.5.1.3. MPPT for Short Circuit Current (SCC)

This technique exerts the PV module's current to calculate the ideal operating current for maximizing power output. The implementation of the algorithm for this offline MPPT approach seems straightforward. Under some arbitrary environmental circumstances, current at MPP (Impp) typically occurs close to short circuit current Isc [65]. One can use Eq. (2.4) to calculate the current at MPP.

$$I_{mpp} = K_i \times I_{SC} \tag{2.4}$$

where the range of factor Ki is 0.75 to 0.9.The aforementioned requirement reveals that this technique is only an approximation and, as a result, is ineffective at definite MPP. Fig. 2.4 illustrates how this strategy is used. This method works well for conditions demanding both high voltage and low current. Moreover, the continuous operation necessitates erratic Isc calculations, which leads to power outages. In reference [66], a novel hybrid approach of SCC with the Perturb and Observe (P&O) method is described. The overall tracking efficiency is increased by this combination, yielding 93.4% and 91.93% in normal and dynamic weather circumstances, correspondingly.

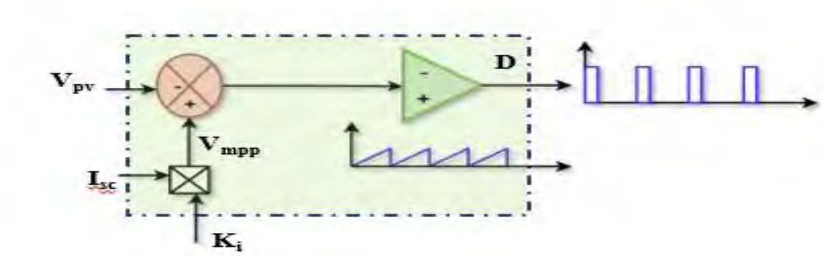

Fig. 2.4: SCC MPPT method schematic block diagram.

2.5.1.4. MPPT for Open Circuit Voltage (OCV)

The open circuit voltage Voc, an off-line parameter that is closer to the Vmpp, is measured by this OCC MPPT, another off-line technique. Eq. (2.5) provides the relationship between (Vmpp) and Voc.

$$V_{mpp} = K_v \times V_{OC} \tag{2.5}$$

In practice, the Kv value falls between 0.7 and 0.8 [51], [53], and can be found using the manufacturer's data sheet. This technique is dependent on projection, as demonstrated in the condition above. Fig. 2.5 illustrates how this method is put into practice.

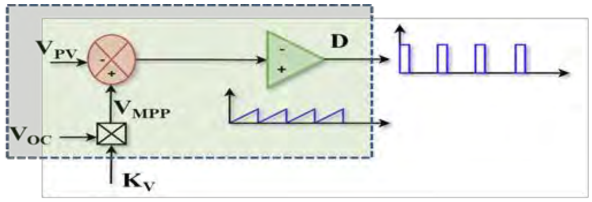

Fig. 2.5. Schematic block diagram of OCV MPPT technique.

As it primarily relies on the rule of approximation, it is best suited for low voltage, high current applications. The uneven measurement of Voc, which leads to needless power use, is the method's downside. A closed-loop controller is utilized to achieve the necessary voltage once the estimated value of Vmpp has been obtained. The PV array actually never functions at the MPP because the connection is merely an estimate. The "smart timer," an enhanced OCV technique developed by A. Frezzetti et al. [67], can also track MPP in PSCs. The frequency of the sample and hold circuit is estimated by this smart timer. This method's hardware implementation is completed, and its efficacy is contrasted with that of traditional OCV.

2.5.1.5. **Hill Climbing Methods (HC)**

This method has a wider use because it works well for low power consumption applications. The LTC1440 Estimator, DG412 Estimator, and NSL-19M51 are utilized. An intelligent timer for sampling and storing the values it is monitoring. The parameter variables employed for the perturbation in this HC approach are voltage (which perturbs the operational voltage) and D (which perturbs the power converter). This method's fundamental idea is to begin with the right initial guess for the solution, which is probably random. Then, using a series of small adjustments to the solution found, the search continues until the best answer is found. The search will be restarted using the same increments if they obtained solution produces another best optimal point. This procedure will keep on till the solution has been improved upon no more. The basic working process for these kinds of strategies is the same for the other ways; however, each one has a different algorithm or set of calculations. This category typically has two methods [68], namely incremental conductance (InC) and perturbs and observes (P&O). A. Ahmed et al. [69] provide a thorough examination of the process of choosing the perturbation's first step, which is an essential consideration for accelerating the convergence of the ideal working point. This technique was implemented using microcontroller Analog-Digital (A-D) converters by W. J. A. Teulings et al. [70].

The perturbation variable is the primary difference between P&O and HC. While the P&O uses voltage as a control variable, the InC primarily relies on the slope of the power-voltage (P-V) curve. The perturbation variable in the HC approach is a D. The most effective and straightforward solution for any microcontroller is the HC method. Additionally, it doesn't require solar PV knowledge or sensors for temperature and radiation. These methods are limited by oscillations around the MPP and their inability to distinguish between power changes caused by changes in G and D.

2.5.1.6. Perturb and Observe (P&O) MPPT

The P&O MPPT is user-friendly due to its straightforward algorithm and ease of implementation on any microcontroller, enabling the majority of authors to adopt it for their applications. According to a literature review, this method depends on the trial-and-error approach for finding and adhering to the MPP [55], [65], and [71]. P&O computation compares the voltage position after comparing the power obtained at two places on a P-V curve. In order to track the MPP, the voltage is then adjusted appropriately, either to the left or right of the P-V curve. Fig. 2.6 displays a block diagram illustration of this P&O approach. This approach essentially looks for changes in PV cell power (dP) before determining the sign of PV cell voltage (dV). D is disturbed based on the values found. The real movement of the operational point is examined using P-V curve data. The actual point appears to be in the left half of the MPP if the (dP=dV) is positive; otherwise, it appears to be in the negative half, depending on the curve. Additionally, this procedure continues until (dP=dV) equals zero.

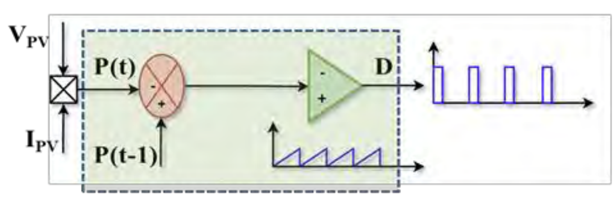

Fig. 2.6. Schematic block diagram of P&O MPPT technique.

Fig. 2.7 displays the algorithm flow chart. MPP can be found at the extreme of any P-V curve using Eq. 2.6 MPP's position (either left or right) is established by applying (Eq. 2.7 and Eq. 2.8.)

$$\frac{dP_{PV}}{dV_{PV}} = 0 = MPP \tag{2.6}$$

$$\frac{dP_{PV}}{dV_{PV}} < 0; \text{ Left side of MPP} \tag{2.7}$$

$$\frac{dP_{PV}}{dV_{PV}} > 0; \text{ Right side of MPP} \tag{2.8}$$

Two sensors are used in the micro-controller-based execution environment to read the PV cell's voltage and current. Citing the work by D. Sera et al. [72], it is found that the MPP may be tracked in 2.5 seconds with an approximate 97.6% tracking efficiency. The DSpace 1103 controller board and the Texas Instruments TMS320F335 controller board are interfaced with Simulink to hardware in this setup. The outcomes show that the efficiencies in both static and dynamic circumstances meet EN 50530 criteria. The most recent advancements in this technique are provided by A. Pandey and S. Srivastava [73].

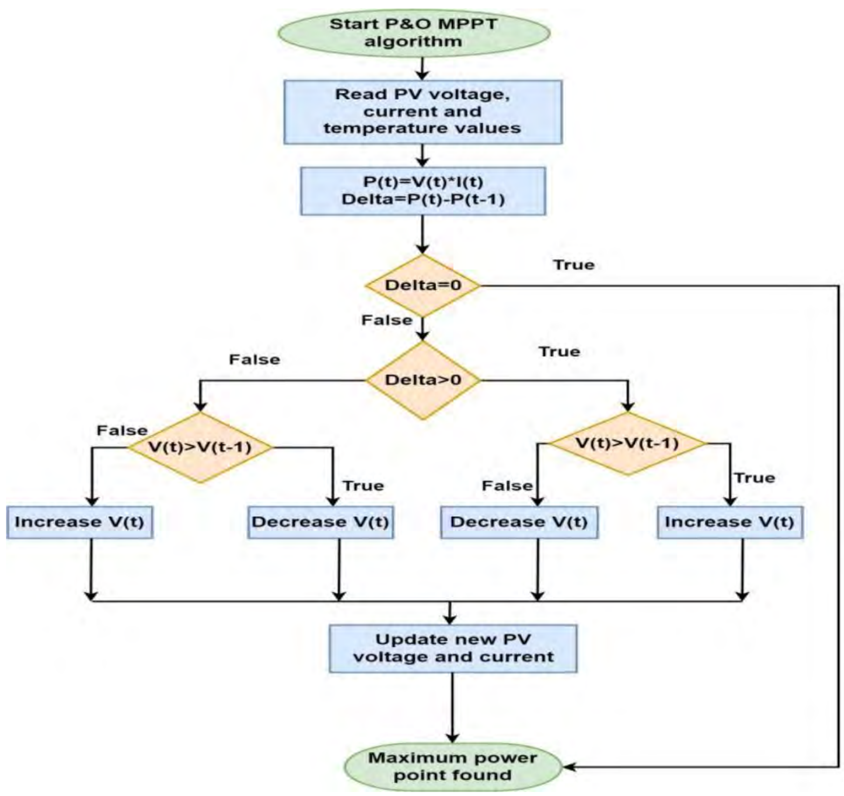

Fig. 2.7. Flowchart of P&O algorithm.

2.5.1.7. Improved Perturb and Observe Method

Unlike traditional P&O, this method avoids needless GMPP following. There is a possibility that the suggested algorithm will require less work to follow the actual MPP. This approach is the refined form of the traditional P&O [74]–[77]. Where Voc is the array's open-circuit voltage, the reference voltage (Vref) is set at roughly 0.8*Voc. They have two modes of operation the first one is voltage search mode and then MPP search mode. The former pushes the operating point closer to the MPP, while the latter aids in determining how accurate the MPP is. First, the peak is monitored using variable/modified P&O computation. When there is a significant likelihood of partial shadowing, the GMPP is monitored. The various adaptive P&O method types were clearly explained by Y. Jiang et al. [78], who also developed a novel MPPT algorithm called the load-current adaptive step-size and perturbation frequency (LCASF) MPPT algorithm. Lastly, a comparison between the LCASF MPPT and traditional P&O was made. According to the investigation, both algorithms track almost as fast and efficiently when the step size perturbation is minor (e.g., 1%). However, the LCASF algorithm's efficiency is 91% when the perturbation is high (e.g., 4%), while the conventional P&O algorithm's efficiency is 88%. By enhancing the elements that lead to losses in conventional P&O, S. K. Kollimalla and M. K. Mishra [79] provided the innovative adaptive P&O. The hardware implementation was completed by N. Khaehintung et al. [80] utilizing a dSPACE30F2010 microcontroller based on FPGA to supply control signals for the forward converter. The PV module Solar MSX-60, which is coupled to a forward converter and runs at a switching frequency of 40 kHz, makes up the system. The two sensors utilized to detect voltage and current from the PV panel are the LV-25 and the Hall sensor LA100. The efficiency of this traditional system is increased to 96% as a result of this development.

2.5.1.8. Incremental Conductance (InC) MPPT

This method basically follows the same procedure as P&O to get MPP, but it makes use of the special relationship found in the I-V curve (current-voltage curve). This computation measures the derivative of PV cell voltage (dV) and current (dI) and comprehends PV cell current and voltage estimations [81]–[83]. The trajectory of the working point is determined by the PV current-voltage curve. It has all the characteristics to be the most well-known one in the literature for uniform conditions because of its medium unpredictability and superior subsequent execution according to P&O approach [84]–[86]. The InC approach relies on the output power P's derivative with respect to the panel voltage V being equal to zero at the MPP. Fig. 10 displays the InC execution technique using the flowchart. With this approach, all of the data will be used to track the MPP using the system's P-V curve's slope. Only the tracking procedure is completed if the P-V curve's slope or the PV array power derivative (dP=dV) is zero. It will be more difficult to monitor MPP while atmospheric circumstances are changing quickly, and the tracking rate will also drop exponentially as a result of the P-V curve's constant shift. Under those circumstances, maintaining the operational point is not very simple. In an effort to extract MPP without oscillations, numerous adaptive step size approaches are being introduced.

Eq. (2.9 – 2.13) provide the mathematical method for determining MPP's location on the P-V curve.

$$P = V \times I \tag{2.9}$$

$$\frac{dP}{dV} = \frac{d(VI)}{dV} \tag{2.10}$$

At the instant of maximum power,

$$\frac{dP}{dV} = 0, \frac{I}{V} + \frac{dI}{dV} = 0 \tag{2.11}$$

To the right of the curve, if the operational point is, then $\frac{dP}{dV} < 0$, the operating point will be on the left side of the curve.

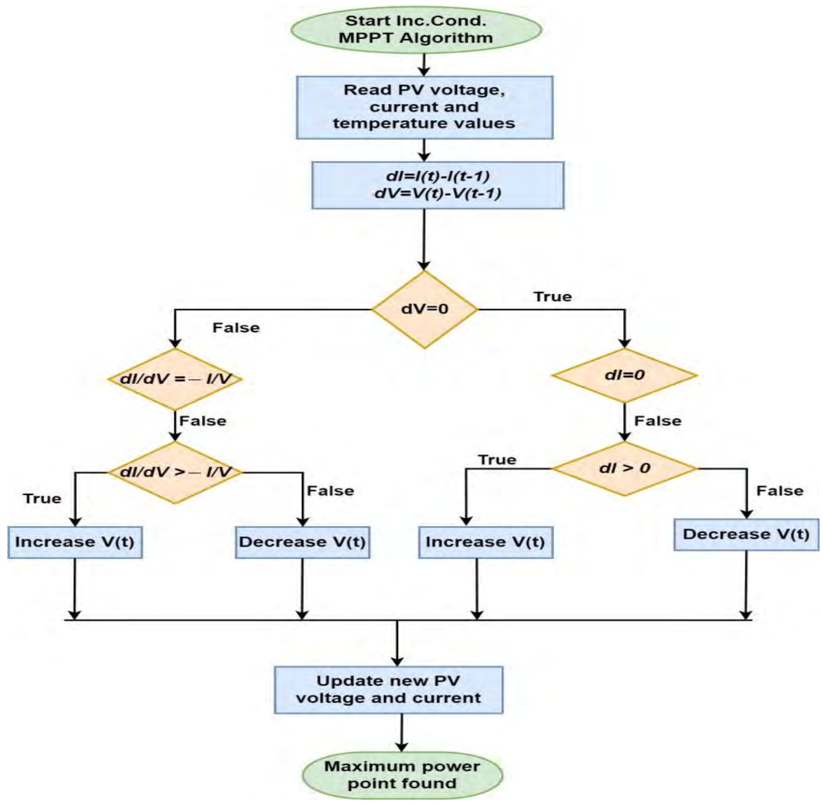

Fig. 2.8. Flowchart of InC algorithm.

$$\frac{I}{V} + \frac{dI}{dV} < 0, \text{ V is decreased} \tag{2.12}$$

$$\text{If } \frac{I}{V} + \frac{dI}{dV} > 0, \text{ V is increased} \tag{2.13}$$

According to reference [60], this controller board strategy has an approximate 98.5% efficiency and can attain MPP in 2.3 seconds. The tracking efficiency increases with the size of the system's increments. Higher increments, however, will cause the system to bounce about the MPP, which also leads to wasteful MPP yielding. The updated InC approach methodologies are provided in the sources [87], [88], and [89]. The hardware implementation of the enhanced InC technique in the TMDS SOLAR EXP KIT (Solar Explorer Kit) C2000 microcontroller environment is provided by P. Sivakumar et al. [90]. The findings demonstrate that tracking is carried out under circumstances where MPPT produces accurate results and that the non-linear loading issue is also addressed. When linked to the grid, both traditional and enhanced approaches are contrasted.

2.5.2. Intelligent MPPT Techniques

2.5.2.1. Fuzzy Logic Controller (FLC)

To increase efficiency, the entire tracking process needs to be enhanced, particularly while tracking in dynamically changing weather circumstances. The PV system must be mathematically modeled for the controller design. It is simpler to model the controller under uniform irradiation circumstances. However, when it comes to PSC design, the issue becomes crucial because the system will be extremely complex. As a result, a clever method that does not call for system mathematical modeling gained attention. Because the controller achieves great efficiency regardless of whether the information is certain or not, trackers that rely on fuzzy logic are thought to be clever. It is not necessary for fuzzy controllers to have an exact scientific model of the PV system. This FLC has two key advantages over other approaches: 1) It does not require a perfect mathematical description of the system, and 2) Only people can build the controller. One of the three main components—the fuzzy rules—are designed using human expertise. Fuzzification, rule base query table (fuzzy rules), and defuzzification are the three steps that make up the fuzzy approach in general [91], [92]. Figure 2.9 illustrates how this method is applied to a solar PV system.

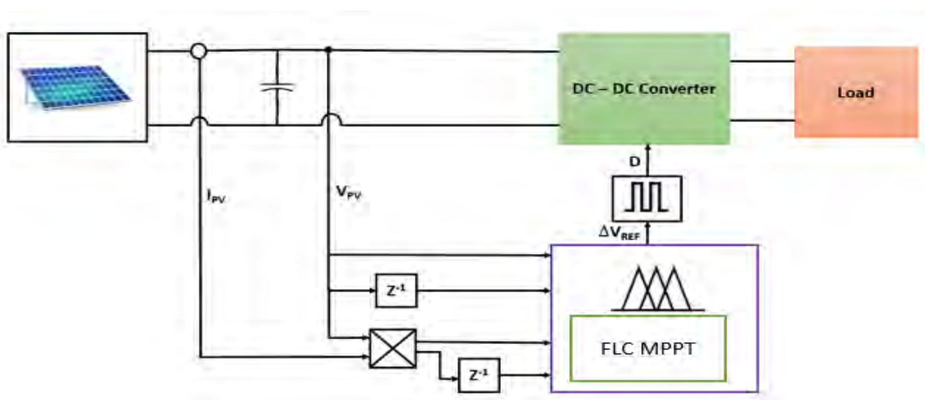

Fig. 2.9. Block diagram of FLC MPPT technique.

Fuzzification is the process of converting the inputs of PV parameters into linguistic variables, or fuzzy sets, from crisp quantities. In order to provide linguistic variables with input and output relationship parameters, if-then rules are primarily created by applying human understanding to design for the proper application need. Defuzzification is an inversion of fuzzification in which linguistic or crisp inputs are extracted using mathematical relations. The centroid method, weighted average method, and maximum membership function are the primary calculation techniques used in this process. During the defuzzification process, the FLC output is transformed from a linguistic variable to a numerical variable, and the converter receives this as an analog signal. The fundamental component of the FLC is the rule basis table, where the approach is adjusted for our application. In order to ensure that the panel voltage is equal to the maximum voltage (V_{mpp}), FLCs operate by continuously changing the D in the converter based on information about changes in error and voltage error. The voltage error is computed by comparing the immediate PV array voltage to the reference voltage. The reference voltage, on the other hand, is the module's maximum voltage for that particular solar radiation moment. In this manner, the sun-powered irradiance indicates variations in the most significant voltage and reference voltage.

$$E(n) = \frac{\Delta P}{\Delta V} = \frac{V_{PV}(n) \times I_{PV}(n) - V_{PV}(n-1) \times I_{PV}(n-1)}{V_{PV}(n) - V_{PV}(n-1)} \quad (2.14)$$

$$\Delta E(n) = E(n) - E(n-1) \quad (2.15)$$

The output of the fuzzy controller, which is the modification in the duty cycle of the converter D, is obtained after ΔE and E are established and switched to the phonetic factors [93], [94]. Fig. 2.10 displays the block-level implementation of FLC. FLC has been shown to function best in dynamic, fluctuating atmospheric conditions. The neuro-fuzzy technique was developed by S. Syafaruddin et al. [95] and illustrates the significance of both distributed MPPT and hybrid techniques. Each array in the 4*3 solar PV setups has a converter. This method tracks the MPP in PSCs more quickly and with extremely high accuracy, but it has the drawback of being more expensive because of the converter placement at each array. The hybrid ANFIS (Artificial Neural Fuzzy Inference System) methodology was presented by N. Priyadarshi et al. [96] in order to increase the system's efficiency and tracking speed. It makes use of dSPACE as the controller's code interface element. Fuzzy cognitive networks are used in the unique MPPT technique presented by T. L. Kottas et al. [97].

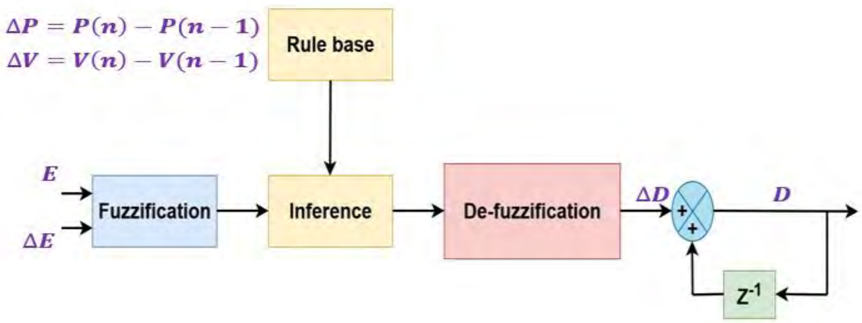

Fig. 2.10. Control block diagram of fuzzy logic controller.

2.5.2.2. Artificial Neural Networks (ANN)

This intelligence-based ANN will be the finest option for handling the most difficult problems. These ANN applications won't need mathematical modeling or in-depth system knowledge. By appropriately mapping the system's input-output, they are able to tackle far more complicated issues in this manner. In essence, the ANN can be seen as a directed chart, with the neurons and synapses serving as the nodes and edges, respectively [98], [99]. Radial basis function networks (RBF) can be used to represent one of the simpler classes of functions.

Figure 2.11 illustrates how these RBF networks relate to the single-layer radial function. The network is made up of n input vector x components that feed to m basis functions.

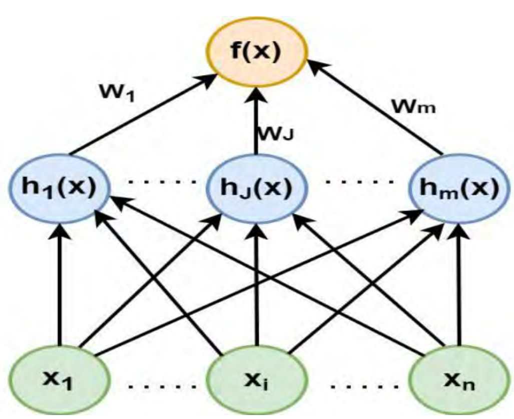

Fig. 2.11. Formulation of neural network

In general, AF is a linear function to nonlinear function converter that includes log-sigmoid and hyperbolic tangent sigmoid. The input, hidden, and output layers—the three primary building blocks of the ANN—are a part of a multi-layer feed-forward system. PV module parameters like

VOC and ISC, environmental data like temperature and irradiance, or any combination of these two can be used as the technique's input. Additionally, the VMPP, Vref, or GMPP will be the output. at order to estimate the best-targeted value, or GMPP, using the available input sets, the procedure is carried out at the most crucial hidden layer and modifies the weights and bias. The learning process and the ANN's structure are both necessary for this technology (ANN) to successfully differentiate the real GMPP. The likelihood that the P-V curve will approach the GMPP increases with the number of data sets (VPV; IPV) at which the P-V curve is evaluated. Unlike previous methods, the ANN's neurons may process information in parallel. The function used in the hidden layers determines how the weights are changed. Additionally, all of the weights are re-initialized simultaneously, providing quick reactions (faster in the process). However, the accuracy of the technique depends on the amount of data. Due to its reliance on PV properties such as module, configurations, and shading, ANN is primarily used in literature in uniform conditions [100]. Therefore, the ANN needs to be re-trained for the system if the setup is changed. To make this ANN function in PSCs, research is still ongoing. PSCs are given the ANN implementation by S. Syafaruddin et al. [95] while taking into account a variety of shading circumstances and configurations. When compared to more traditional methods like P&O and InC, this strategy produces better results in those PSCs. The elements to be taken into account when designing the ANN for PSCs are described in depth in References [101], [102].In Fig. 2.11, the ANN is implemented in detail. To anticipate real-time issues, T. Himaya et al. [103] show how to choose PV panels for the effective application of this ANN approach. Using the ANN methodology, M. A. Younis et al. [104] developed the enhanced MPPT technique. This ANN approach is simulated by A. K. Rai et al. [105] while taking changeable PV parameters into account. Hardware implementation of this technique involves a cheap calculation-based controller with the best AF in the model, and it is simpler to build in a small micro-controller with low costs.As a result, computations are completed much more quickly, which leads to a rapid rate of convergence towards the output. The hybrid GA-ANN based MPPT technique was modeled by A. A. Kulaksız and R. Akkaya [106], who produced tracking MPP more quickly. The two conference papers that provide the RNN-based ANN technique tracking under varied meteorological conditions are references [107], [108]. An overview of these artificial intelligence methods can be found in reference [109].

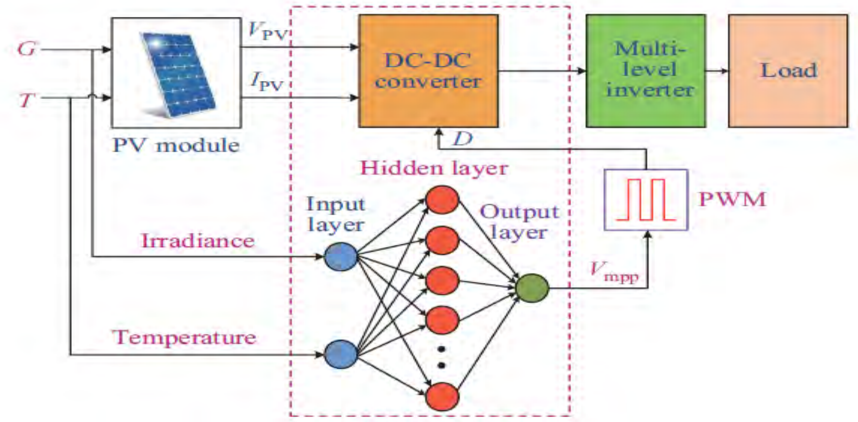

Fig. 2.12. Detailed implementation of ANN method.

2.5.2.3. Sliding Mode Controller (SMC)

The most crucial element for any controller is the convergence process. In particular, this procedure will take longer if there are unanticipated disruptions or sudden changes. An extremely advanced intelligence-based SMC is made to follow the MPP rapidly without sacrificing effectiveness. The methodology's fundamental notion is to sense the DC link capacitor's current in order to operate the DC-DC converter. There are two ways that this system can work: sliding mode and approaching mode [110]. Three modes—traversability, reachability, and comparable control—are used to characterize the sliding mode process flow. First, the application must determine which sliding surface is best. The system's non-linear properties are managed by this non-linear approach.The primary benefit will be that this technique is independent of the PV array and configuration size. Particularly when integrated into the grid, this non-linear method reduces the ripple generated by the converter and tracks the MPP quickly and robustly. It makes use of the control equation to ensure that the system parameters remain on the sliding surface regardless of source side changes. Because it only uses one current sensor, the system's overall cost is decreased. The design elements of the sliding surface are explained in detail by S. Tan et al. [111]. This approach is based on calculating the difference between PV power and PV voltage, which is done using the Eq. (2.16)

$$E(n) = \frac{\Delta P}{\Delta V} = \frac{V_{PV}(n) \times I_{PV}(n) - V_{PV}(n-1) \times I_{PV}(n-1)}{V_{PV}(n) - V_{PV}(n-1)} \qquad (2.16)$$

$$\Delta E(n) = E(n) - E(n-1) \tag{2.17}$$

$$S = \frac{dP_{PV}}{dV_{PV}} = I_{PV} + V_{PV} \times \frac{dI_{PV}}{dV_{PV}} \tag{2.18}$$

where S will determine the precise operating voltage value based on the MPP's area using Eq. (2.18). Furthermore, Fig. 2.13 provides the step-by-step flow process for the hardware implementation-based SMC technique. Therefore, the aforementioned approach governs the DC/DC converter [112], [113]. The DCDC converter is primarily controlled in a hysteretic mode using this technique. Although it is quick, the converter that is being used has an unsteady switching frequency. Operation converges to the MPP in a few tens of milliseconds, according to simulation and experimental results [114]. This current sensing algorithm was implemented on hardware using the P&O technique by E. Bianconi et al. [115].Without the need for an extra feedback loop, the 100 HZ voltage oscillation noise was effectively eliminated in this implementation. Thus, with this hybrid combination, SMC offers the finest MPP tracking. An innovative fast current-based SMC approach is presented by E. Bianconi et al. [116].

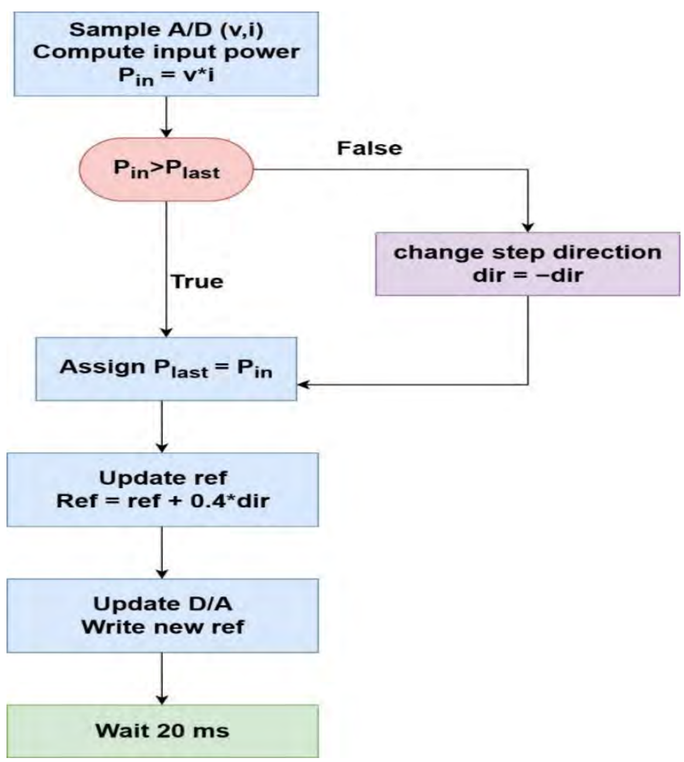

Fig. 2.13. Flowchart of sliding mode controller.

2.5.2.4. Gauss- Newton Approach Based MPPT

The primary significance of this Gauss-Newton method is its theoretical efficiency in comparison to other methods found in the literature. It will use the more recent center differentiation technique to find the MPP. The quickest of these mathematical computational MPPT methods is the Gauss-Newton approach. It bears the names of two renowned scientists, Isaac Newton and Carl Friedrich Gauss. Its primary function is to resolve nonlinear issues related to the least squares approximation. It should minimize the sum of a squared value of that specific objective function since it is a variation of the Newton approach. The fundamental tenet of this approach is that the second-order derivatives, which are extremely difficult to solve, do not need to be calculated. By accurately estimating the function's initial guess values, this kind of clever approach lowers the number of iterations. Therefore, while choosing these algorithms for unconstrained minimization, there should be a trade-off between computation/memory and the number of iterations [51], [117], and [118]. The objective of the Gauss-Newton approximation is to break down the objective function f = L*m into two primary categories:

i. Regression function or vector-based model.

ii. Scalar valued loss, like the sum squared difference between the target value (l) and the expected output.

Therefore, with the aid of (2.19), (2.20), and (2.21), the mathematical analysis is used to express the objective function.

$$m_i = y_i - r(t_i, X) \quad (y_i, t_i) \quad i = 1,2, \ldots., P \tag{2.19}$$

$$f(x) = \frac{1}{2}\sum_{i=1}^{P}(y_i - r(t_i, X))^2 \tag{2.20}$$

$$\text{i.e} \quad l = \sum((m_i)^2) \tag{2.21}$$

Applying this technique to non-linear systems has advantages. This approach effectively solves extremely complicated equations, and [119] provides advances in their computations. In their extensive simulations, A. M. Farayola et al. [120] compared the CGSVM (coarse-Gaussian support vector machine) and used the Gauss-Newton technique. The new approach is contrasted with the three MPPT methodology types (ANN, ANFIS, and ANN-P&O).

2.6. Summary

The main limitations of PV systems and the crucial role MPPT approaches play in overcoming them have been covered in detail in this paper. The investigation compared sophisticated techniques that provide greater flexibility in dynamic situations with conventional algorithms, which are prized for their simplicity. The trade-off between tracking performance and computing complexity was found to be quite evident. As a result, there is a research void for a technique that strikes a balance between high efficiency and robustness. The innovative MPPT method created in the following chapter is explicitly justified by this deficiency.

Chapter 3

Methodology: The Proposed MPPT Algorithm

This chapter describes the comprehensive methodology underpinning the proposed Sweep Assisted Enhanced Adaptive Fuzzy Perturb and Observe (P&O) Maximum Power Point Tracking (MPPT) algorithm. The system architecture, the mathematical models of the core components, the novel control strategy, and its implementation in a MATLAB/Simulink environment are thoroughly expounded.

3.1. System Modeling

The photovoltaic (PV) generation system under study consists of a 100 kW array, a boost DC–DC converter, and an adaptive MPPT controller. The PV array is configured with 40 parallel strings, each containing 10 series modules. The converter employed is a boost topology with inductance L=1mH and capacitance C_1=2.5mF. This topology ensures the PV voltage is stepped up to match the required DC bus level. The duty cycle of the switch, denoted as D, is dynamically adjusted by the MPPT algorithm to force the PV array to operate close to its maximum power point (MPP). Environmental dependencies such as irradiance (G) and temperature (T) are incorporated in the control model. Temperature influences the open-circuit voltage via a negative coefficient (−0.31∘C), while irradiance determines the photocurrent. These relations are embedded into the MPPT logic through estimated voltage thresholds.

3.1.1. Photovoltaic Array Model

The PV array is constructed by connecting several modules in series-parallel configuration to achieve the desired power rating. The fundamental equation governing the I-V characteristics of a PV cell is given by the single-diode model [1]:

$$I = I_{ph} - I_O[\exp\left(\frac{q(V + IR_S}{nkT}\right) - \frac{V + IR_S}{R_{sh}} \qquad (3.1)$$

Wehre,

I and **V** are the output current and voltage of the cell, respectively,

I_{ph} is the photocurrent, proportional to solar irradiance (G),
I_0 is the reverse saturation current of the diode,
q is the electron charge (1.602×10^{-19}C),
k is the Boltzmann constant (1.381×10^{-23} J/K),
T is the junction temperature in Kelvin,
n is the diode ideality factor,
R_s and R_{sh} are the series and shunt resistances, respectively.

For the proposed system, a large-scale array is modeled using the parameters derived from the code: 40 parallel strings, each string comprising 10 series-connected modules. Each module has an open-circuit voltage V_{oc}=37.2 V and a voltage at maximum power Vmp=30.1 V. Consequently, the array's cumulative characteristics are:

Array Open-Circuit Voltage, $V_{oc,array}$ = 372 V
Array Voltage at MPP (Nominal), $V_{mpp,array}$ = 301 V
Array Maximum Power, $P_{max,array} \approx$ 100, kW
The model accounts for the effects of varying irradiance and temperature on these parameters. The temperature coefficient of V_{oc} (β=−0.31/°C) is used to adjust the estimated MPP voltage.

3.1.2. DC-DC Boost Converter Model

The DC-DC boost converter is the fundamental power processing unit in this MPPT system. Its primary function is to draw power from the PV array at the voltage determined by the MPPT algorithm and efficiently step it up to a higher, regulated DC-link voltage, which is suitable for inversion to the grid or for supplying a high-voltage DC load. The converter's operation is governed by the switching action of a semiconductor device (typically an IGBT or a MOSFET for this power level), which controls the energy transfer from an inductor to the output capacitor and load.

The analysis assumes the converter operates in Continuous Conduction Mode (CCM), where the inductor current never falls to zero within a switching period. This is a valid and necessary assumption for a high-power system to minimize peak currents and reduce current stress on components.

3.1.2.1. Governing Equations and Waveforms

The operation of the boost converter can be broken down into two distinct switching states within one period T_s, where D is the duty cycle and $t_{on} = DT_s$ is the interval when the switch is ON, and $t_{off} = (1-D)T_s$ is the interval when the switch is OFF and the diode is conducting.

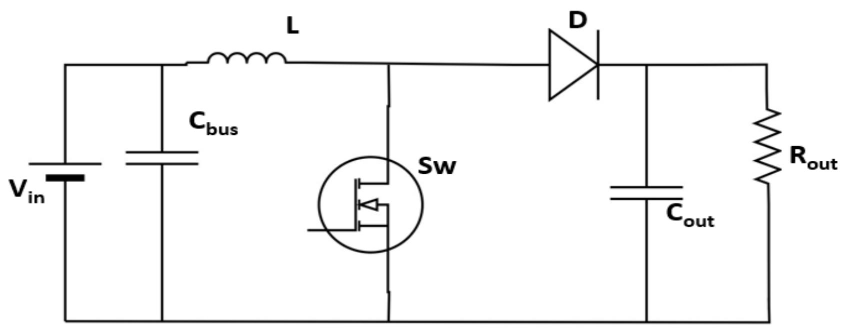

Fig. 3.1. Circuit diagram for boost converter.

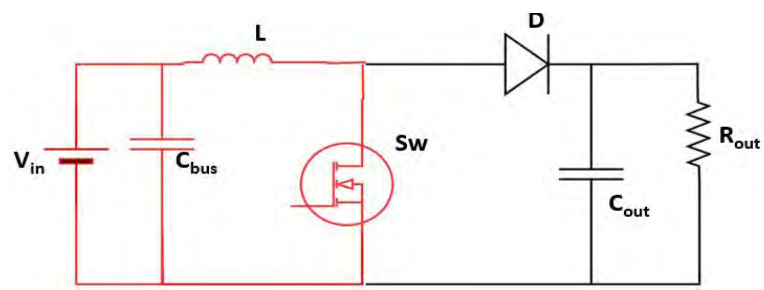

Fig. 3.2: Circuit diagram for On-state operation of boost converter.

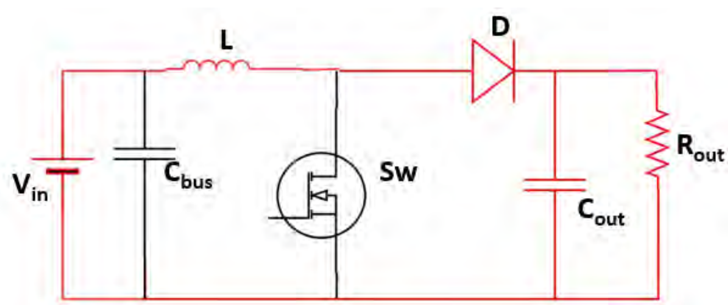

Fig. 3.3. Circuit diagram for Off-state operation of boost converter.

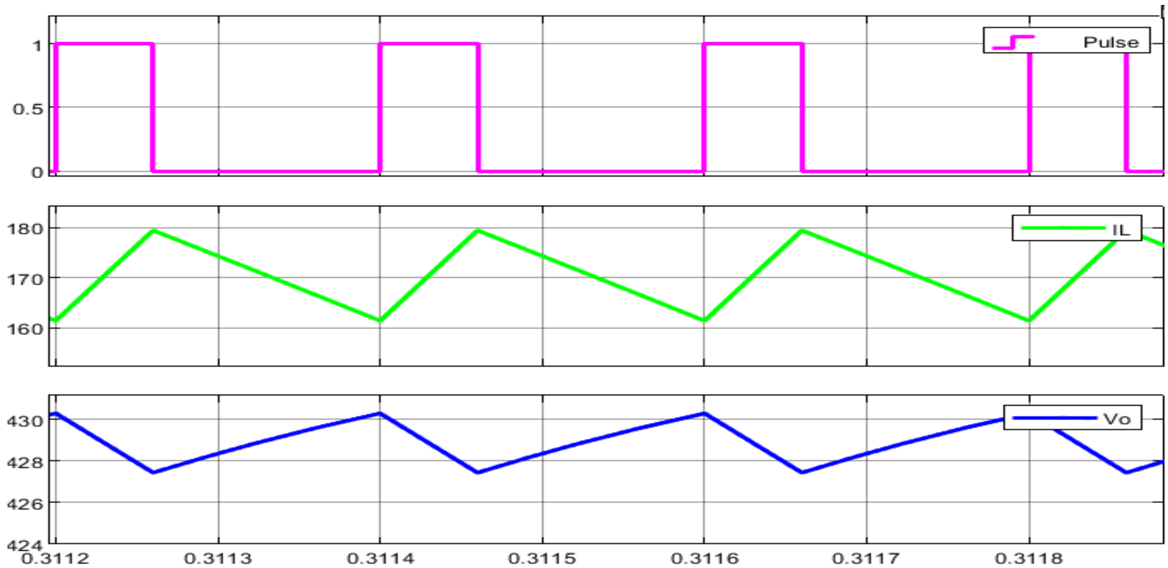

Fig. 3.4. Waveforms for inductance current ripple and capacitor voltage ripple.

During this state, the switch is closed. The diode becomes reverse-biased by the output voltage, isolating the output stage. The input PV source charges the inductor, causing its current to ramp up linearly. The output capacitor supplies energy to the load.

$$\Delta i_{L(on)} = \frac{V_{pv}.DT_S}{L} \tag{3.2}$$

During this state, the switch is open. The inductor current must continue to flow, forward-biasing the diode. The energy stored in the inductor is transferred, along with power from the PV source, to the output capacitor and the load. The inductor current decreases linearly.

$$i_{L(off)} = \frac{\left(V_{pv} - V_{out}\right).(1-D)T_s}{L} \tag{3.3}$$

For steady-state operation, the net change in inductor current over one complete switching period must be zero:

$$\Delta i_{L(on)} + \Delta i_{L(off)} = 0$$

Substituting the expressions from Eq. 3.2 and Eq. 3.3 the following expression can be written

$$\frac{V_{pv}.DT_s}{L} + \frac{(V_{pv} - V_{out}).(1-D)T_s}{L} = 0$$

Solving for V_{out} yields the fundamental input-output voltage relationship of the ideal boost converter:

$$V_{out} = \frac{V_{pv}}{1 - D} \tag{3.4}$$

The ideal input-output power relationship, assuming 100% efficiency, is:

$$P_{pv} = P_{out} \rightarrow V_{pv}.I_{pv} = V_{out}.I_{out}$$

Therefore, the output current is:

$$I_{out} = I_{pv}.(1 - D) \tag{3.5}$$

3.1.2.2. Component Sizing and Design Considerations for a 100 kW System

The practical design of the boost converter must account for non-ideal components and specify values for L and C based on allowable ripple and switching frequency.

The inductor value is chosen to limit the peak-to-peak inductor current ripple (ΔI_L) to a specified percentage of the maximum average input current. A typical design choice is a ripple between 20-40% of the maximum current. This represents a trade-off between size (smaller L) and conduction losses (larger L).

The current ripple is derived from the ON-state equation:

$$\Delta I_L = \frac{V_{pv}.D}{f_{sw}.L} \tag{3.6}$$

where $f_{sw}=1/T_s$ is the switching frequency.

Rearranging to solve for the required inductance:

$$L = \frac{V_{pv}.D}{\Delta I_L.f_{sw}} \tag{3.7}$$

The output capacitor is sized primarily to limit the output voltage ripple (ΔV_{out}) to an acceptable level, typically 1-2% of the output voltage. The worst-case ripple occurs when the converter is supplying a constant load current I_{out} and the capacitor must supply the entire load current during the switch ON interval.

The charge removed from the capacitor during t_{on} is:

$$\Delta Q = I_{out}.t_{on} = I_{out}DT_S \quad (3.8)$$

This charge removal causes the voltage ripple:

$$\Delta V_{out} = \frac{\Delta Q}{C} = \frac{I_{out}.D}{f_{SW}.C} \quad (3.9)$$

Rearranging to solve for the required capacitance:

$$C = \frac{I_{out}.D}{\Delta V_{out}.f_{SW}} \quad (3.10)$$

The tracking efficiency equation for the solar cell has been considered as follows:

$$\eta_{MPPT} = \frac{\int_0^t P_{out}(t)dt}{\int_0^t P_{max}(t)} \quad (3.11)$$

3.2. Proposed MPPT Algorithm

The proposed control method is a sweep assisted enhanced adaptive fuzzy perturb-and-observe (P&O) scheme. It integrates three core stages:

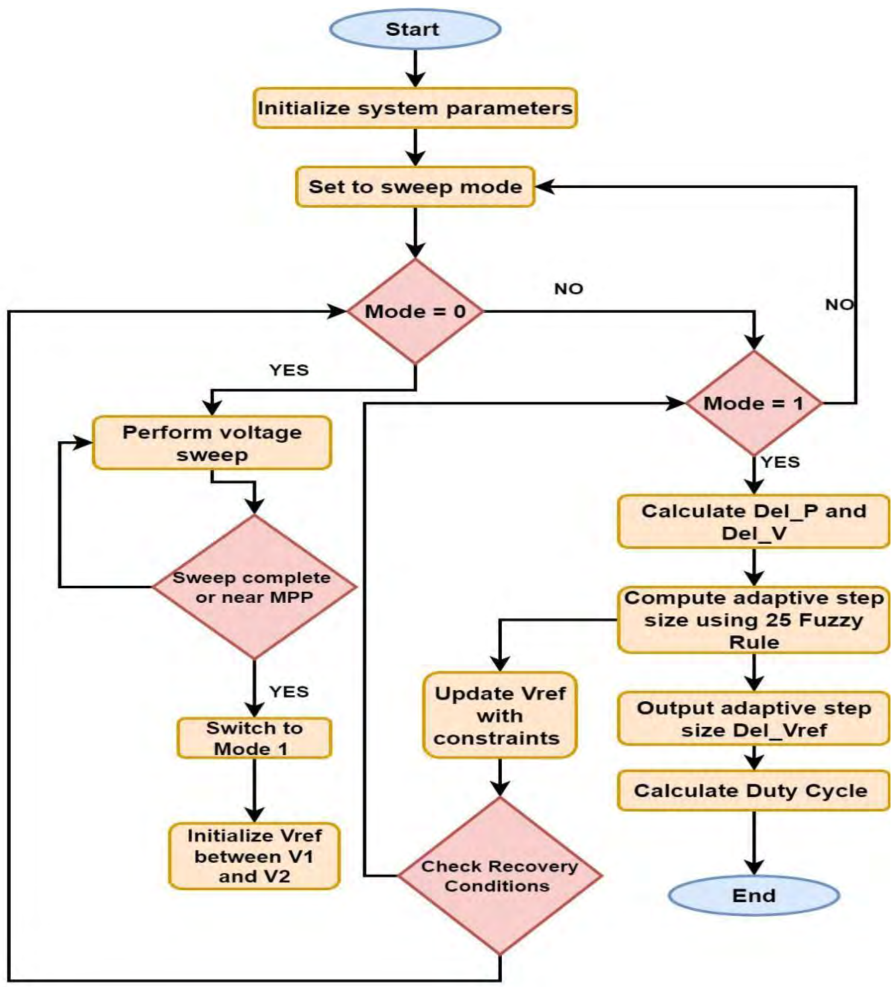

Fig. 3.5. Flowchart for proposed algorithm.

3.2.1. Sweep Mode:

The algorithm initiates in Mode 0. This mode is designed to rapidly bring the operating point into the area of the Global Maximum Power Point (GMPP), especially crucial after startup or a major environmental disturbance. At startup, the system enters a sweep phase. The duty cycle is incremented stepwise, scanning the operating region. The sweep continues until the estimated duty corresponding to the expected V_{mpp} is reached. A counter monitors the number of sweeps; if convergence is detected, the controller transitions to fuzzy mode. This guarantees fast initialization and avoids mis-tracking after abrupt irradiance changes.

The duty cycle (D) is perturbed with a fixed step size sweep step =0.02. This sweeps the operating point across the entire I-V curve. Simultaneously, an initial estimate of the MPP voltage ($V_{mpp,est}$) is calculated using an empirical formula that incorporates real-time measurements of average irradiance (G_{avg}) and temperature (T):

$$V_{mpp,est} = V_{mpp,array} \, . \left(1 + \beta(T - 25)\right) . \left(1 + 0.05 \, . \ln\left(\frac{\max(G_{avg}, 100)}{1000}\right)\right) \quad (3.12)$$

This estimate is bounded within practical limits (50 V to $0.95 \cdot V_{oc,array}$). The sweep counter (sweep counter) increments if the operating point is far from the estimated MPP. After a predefined number of sweeps (sweep counter)>=6, the algorithm transitions to Mode 1. The initial reference voltage (V_{ref}) for Mode 1 is set within a defined voltage band around $V_{mpp,est}$.

3.2.2. Fuzzy Logic–Based Fine Tracking:

Once the system is near the expected MPP, a fuzzy controller refines the reference voltage V_{ref}. This is the core operational mode, where a Fuzzy Logic Controller (FLC) replaces the conventional fixed-step P&O perturb mechanism. The inputs to the FLC are the instantaneous changes in power $\Delta P = P_{pv}(k) - P_{pv}(k-1)$ and voltage ($\Delta V = V_{pv}(k) - V_{pv}(k-1)$. These inputs are normalized to the range [-1, 1] to ensure the fuzzy rule base remains general and effective across the operating range.

Each normalized input is mapped to five fuzzy sets using trapezoidal membership functions: Negative Big (NB), Negative Small (NS), Zero (ZE), Positive Small (PS), and Positive Big (PB). A 5x5 rule matrix, shown in Table 3.1, defines the relationship between input fuzzy sets and the output, which is the adaptive step size for the voltage reference (ΔVref). The rules are designed to produce a large step change when the operating point is far from the MPP (ΔP is large) and a very small step when it is near the MPP (ΔP is small or zero) to minimize oscillations. Table 3.1 shows the Fuzzy rule used for the proposed algorithm.

Table 3.1. Fuzzy rules used for proposed method

ΔV \ ΔP	NB	NS	ZE	PS	PB
NB	VS	VS	VS	S	S
NS	VS	VS	S	M	M
ZE	VS	S	M	L	L
PS	S	M	L	VL	VL
PB	S	M	L	VL	VL

The centroid method is used to convert the aggregated fuzzy output into a crisp value for ΔV_{ref}.
A critical enhancement is the imposition of dynamic voltage constraints on the reference voltage. The boundsV_1 and V_2 (e.g., 290 V and 310 V for a nominal 301 V MPP) are scaled based on the real-time Vmpp,est. This prevents the algorithm from searching inefficient regions of the I-V curve (e.g., near open-circuit or short-circuit conditions), significantly improving dynamic response and stability.

$$\text{Current\_}V_1 = V_1.(V_{mpp,est}/\ V_{mpp,array}) \tag{3.13}$$

$$\text{Current\_}V_2 = V_2.(V_{mpp,est}/\ V_{mpp,array}) \tag{3.14}$$

A recovery mechanism monitors for conditions indicating that the operating point is stuck at a constraint boundary without achieving maximum power (V_{pv} >= Current_V_2& $\Delta P < 0$). If this persists, the algorithm triggers a return to Mode 0 for a global re-sweep, ensuring robustness against trapping at local maxima or during severe transients.
The final duty cycle is calculated using a proportional controller that adjusts the previous duty cycle to minimize the error between the PV voltage (V_{pv}) and the fuzzy-determined optimal reference voltage (V_{ref}).

$$D(k) = D(k-1) + K_p.\frac{(V_{ref} - V_{pv})}{V_{oc,array}} \tag{3.15}$$

where K_p is a proportional gain. The duty cycle is clamped between 0.05 and 0.95 to ensure the boost converter operates within its safe limits.

3.3. Implementation in Simulink

The entire system, comprising the PV array model, the boost converter with its switching logic, and the proposed MPPT algorithm, is implemented in MATLAB/Simulink. The MPPT algorithm is encapsulated within a MATLAB Function block, facilitating code-based design and integration with the Simulink graphical environment. The algorithm executes at a defined sampling interval (Ts), which is chosen to be slower than the converter's switching frequency to allow the system to settle between perturbations, yet fast enough to track environmental changes. The function output includes a debug vector containing key internal variables ($V_{mpp,est}$, $\Delta V_{ref,}$ mode, Current_V_1, Current_V_2). This allows for real-time monitoring and performance validation through Simulink scopes and displays, which is included in the results and analysis section.

In summary, the proposed hybrid algorithm leverages an initial global sweep for a rough location of the MPP, followed by a highly efficient, constrained, and adaptive fuzzy P&O search for precise tracking. The integration of voltage constraints and a recovery mechanism ensures both speed and robustness, making it particularly suitable for large-scale PV systems where efficiency and stability are paramount.

3.4. Simulation results for Fuzzy rule based output curves

The trapezoidal membership functions are defined for the inputs (ΔP and ΔV) and uses a Sugeno-type fuzzy rule base to compute the output adjustment step (ΔVref). The following plots in Fig. 3.6 represents input and output membership degree for input and output of Fuzzy Inference System.

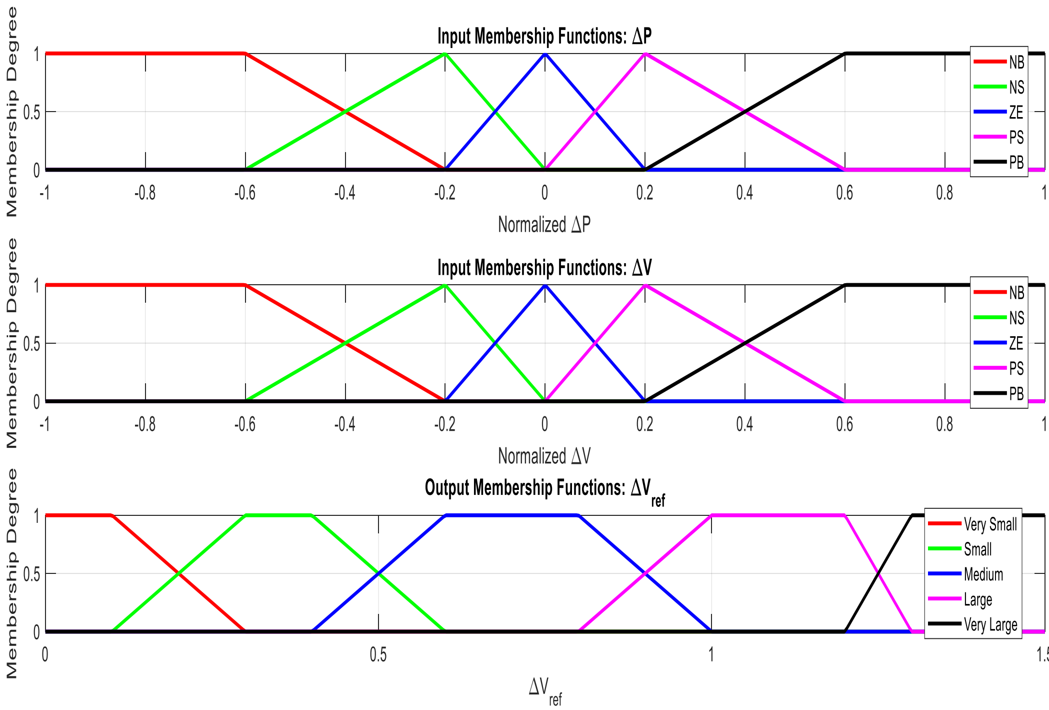

Fig. 3.6. Plot for designed Membership degree of ΔP, ΔV and ΔV_{ref}

A 3D surface and Fuzzy Logic ΔVref contour showing how the fuzzy rules map input changes to output step sizes are shown in Fig. 3.7 (a) and (b). Additional figures show rule activation levels for a specific operating point, the dynamic adaptation of ΔV_{ref} over time under varying ΔP and ΔV, and both 3D and heatmap representations of the rule table itself. Together, these visualizations provide a detailed understanding of how the fuzzy MPPT controller adapts its step size, activates different rules, and converges toward the maximum power point under different operating conditions.

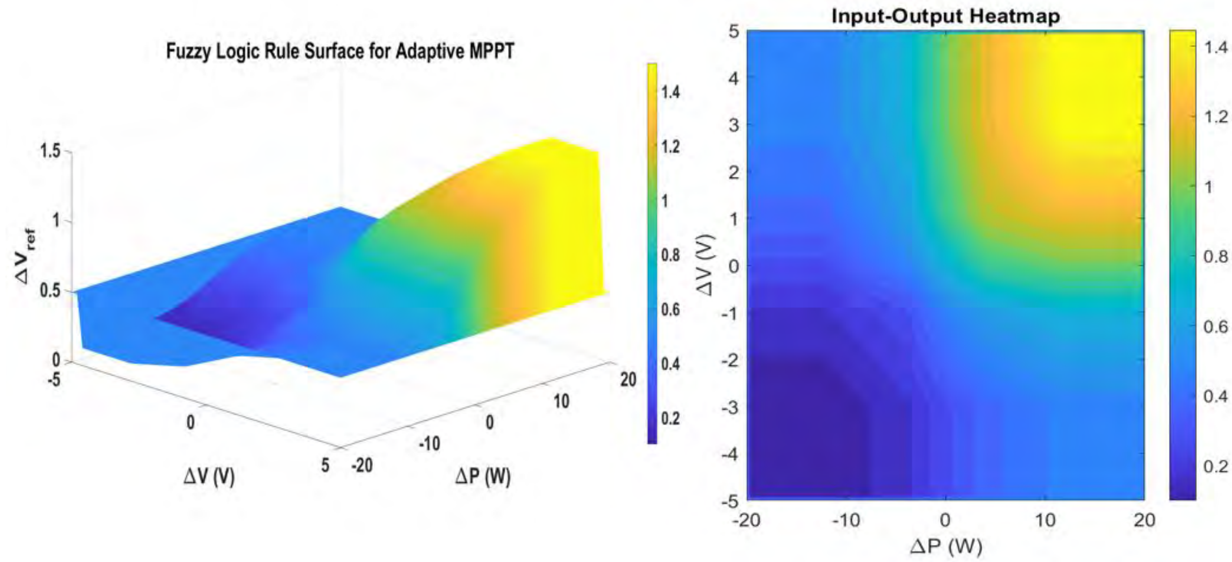

(a) (b)

Fig. 3.7. Comparative plots of (a) 3D surface and (b) Fuzzy Logic ΔVref contour for fuzzy MPPT controller

The first plot in Fig 3.8 (a) is 3D surface plot, where the axes represent the input linguistic variables—change in power (dP) and change in voltage (dV)—mapped to their fuzzy levels (NB, NS, Z, PS, PB). The height of the surface corresponds to the output adjustment of the reference voltage (ΔVref). This surface highlights how the fuzzy controller responds to different input conditions, with smooth gradients showing how ΔVref increases from small corrections (e.g., 0.1) to larger adjustments (up to 1.5). The second plot in in Fig 3.8 (b) is a 2D heatmap, which flattens the same rule table into a color-coded matrix. Here, the colors reflect the output intensity, and each cell is annotated with the exact numerical value of ΔVref, making it easier to read precise rule consequences.

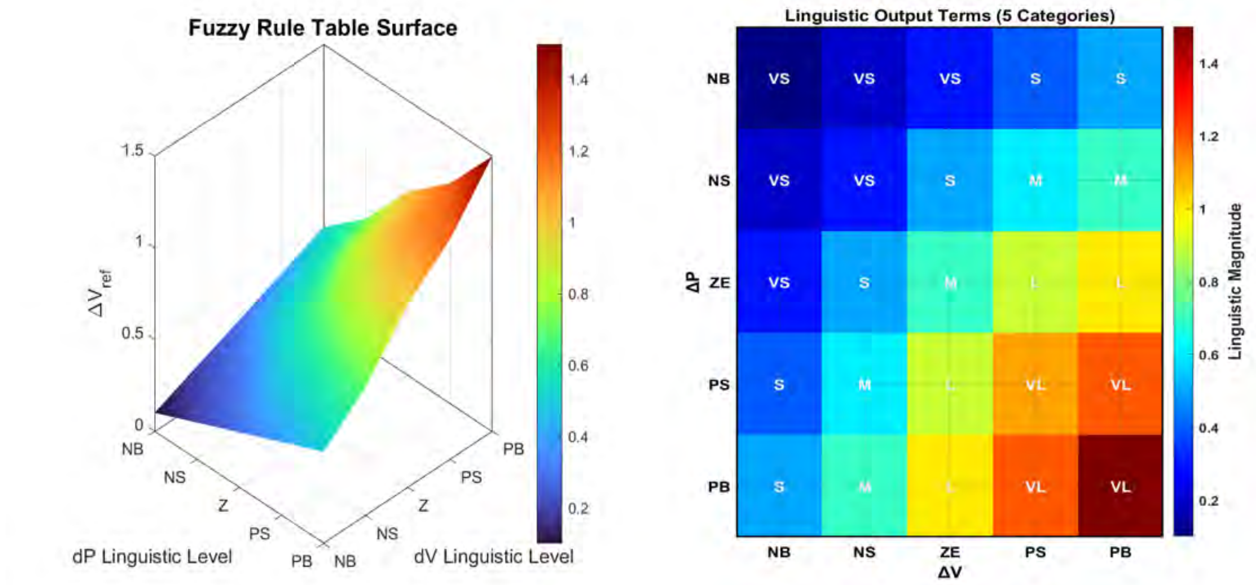

(a) (b)

Fig. 3.8. Comparative plots of (a) 3D Fuzzy Rule Surface and (b) Fuzzy Rule Heatmap for fuzzy MPPT controller

Chapter 4
Results and Discussion

4.1. Steady-State Performance

The steady-state performance of the proposed algorithm is significantly better than the traditional P&O, InC, and Modified P&O approaches which can be observed on the zoomed view in Fig. 4.1. The proposed approach (green) converges to the maximum power point (MPP) with a settling time of around 0.28 seconds under constant irradiance of 700 W/m². This is about 60% faster than the 0.38 seconds needed by the P&O method (blue). More significantly, the suggested method shows almost no power oscillation at steady state, with a ripple size of less than 0.5% of the rated power. On the other hand, the InC (yellow) and Modified P&O (red) approaches show smaller but still significant ripples of 2.8% and 3.2%, respectively, while the P&O method displays a continuous oscillation with a peak-to-peak ripple of about 4.5%. This shows that the suggested hybrid strategy achieves both fast convergence and remarkable stability by effectively decoupling the basic trade-off between tracking speed and steady-state oscillation.

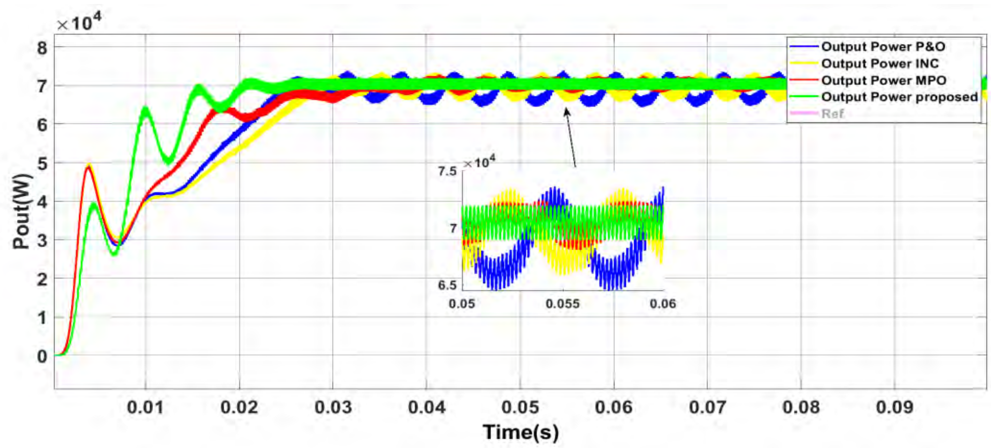

Fig. 4.1. The output power response for 700W/m^2.

Voltage curve for static irradiance is shown in Fig 4.2, the proposed algorithm shows 0.6V whereas the modified P&O shows 10.2V P&O illustrates 40V and InC with 31.7V. In Fig 4.3 the duty cycle response are compared for the static irradiance, where it can be clearly seen that the proposed algorithm works better than the other conventional methods. At the beginning the duty cycle oscillates around the desired value and then goes to the steady state condition and in case of the other methods the duty cycle takes time to go to the stable region. In Fig 4.4 Change in Pout, Vpv and Duty Cycle with Mode Transition is shown for static irradiance of 700W/m^2. Mode 0 occurs at the beginning as the desired voltage is sensed Mode 1 is selected.

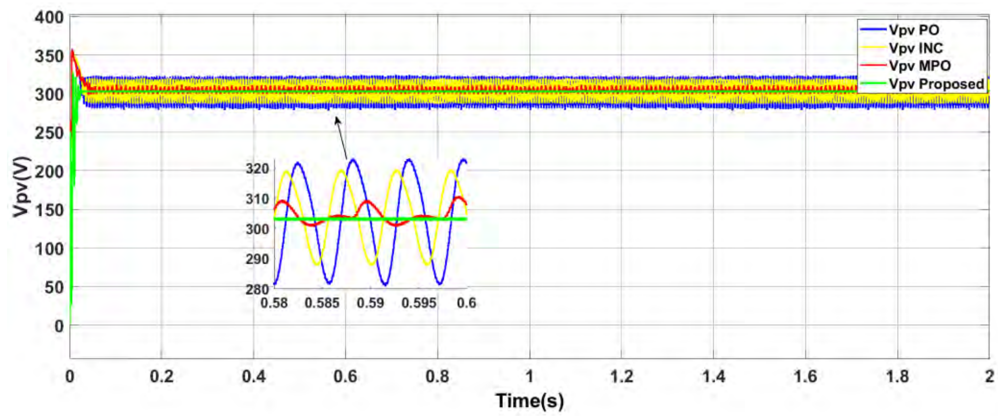

Fig. 4.2. Voltage curve for static irradiance of 700W/m^2

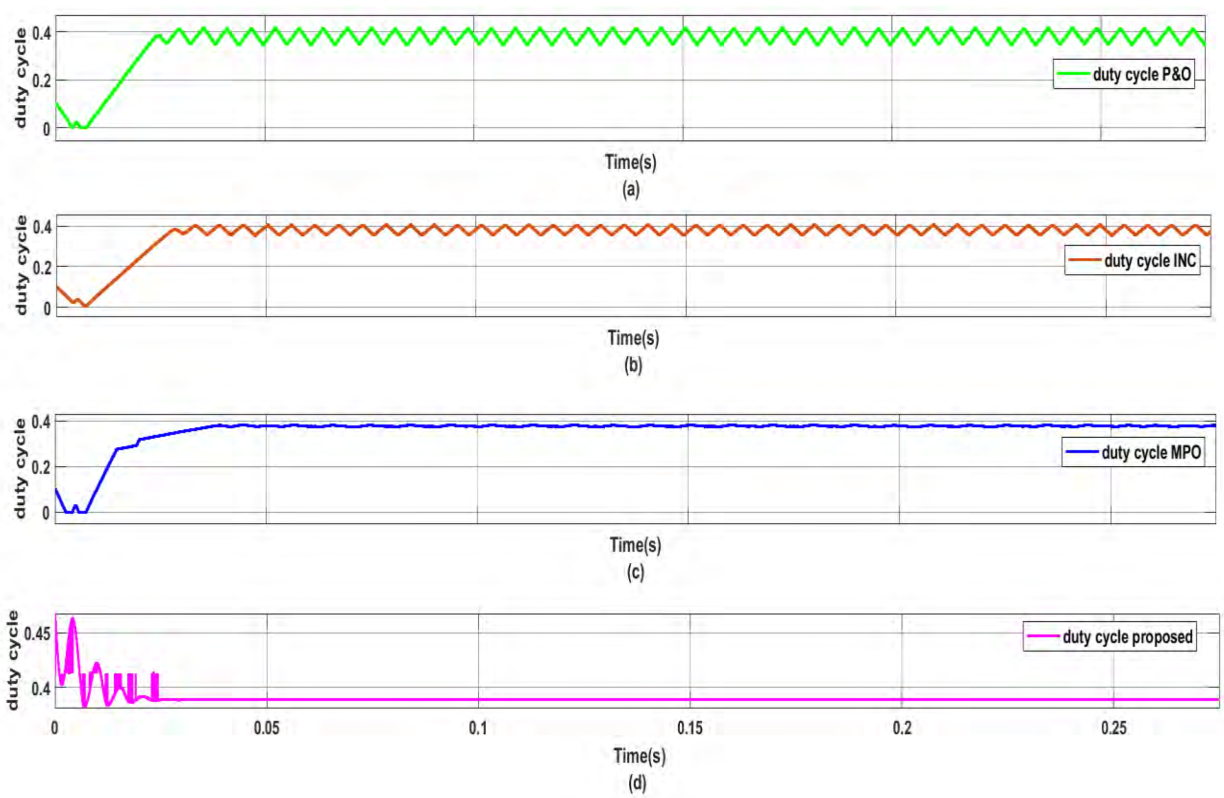

Fig. 4.3. Duty cycle curve for static irradiance of 700W/m^2

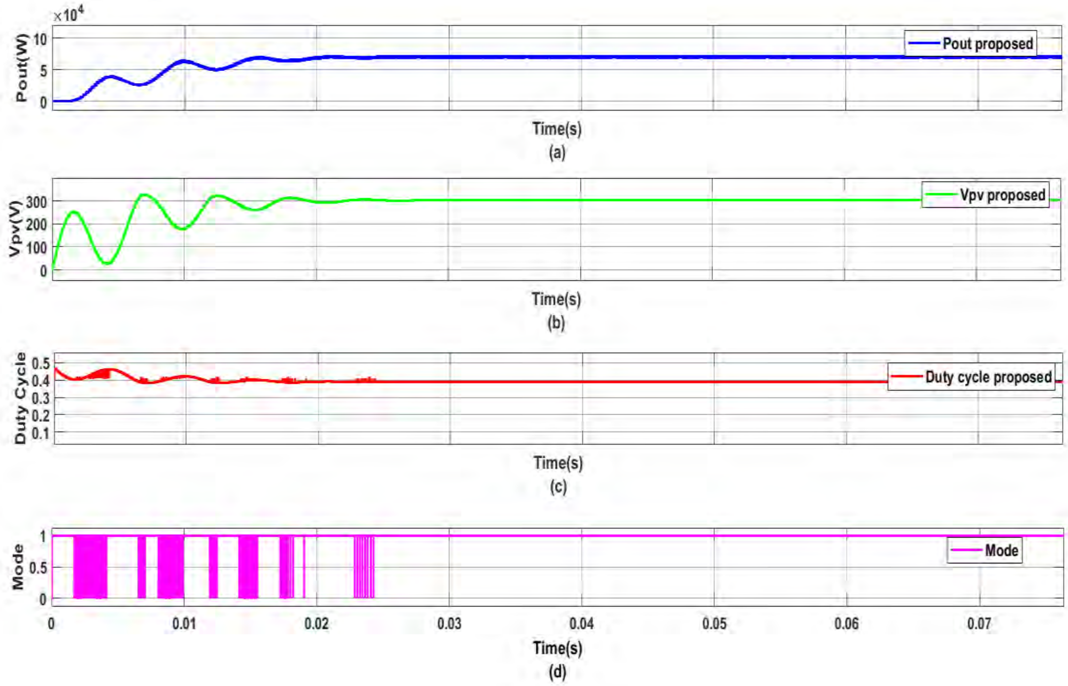

Fig. 4.4. Change in P_{out}, V_{pv} and Duty Cycle with Mode Transition for static irradiance of $700W/m^2$

As shown in Table 4.1 the proposed algorithm performs better than the other conventional methods at static irradiance. The tracking efficiency is obtained 99.01% for the proposed algorithm whereas 98.1% is for the modified P&O and 98% and 97% is for the P&O and InC respectively. The voltage oscillation for the proposed algorithm is found 0.6V which is extremely good response than the other conventional methods

Table 4.1. Performance analysis for different MPPT methods for static irradiance of $700W/m^2$

Algorithm	Tracking Efficiency	Voltage Oscillation	Power Oscillation	Output Power	Tracking Speed
Proposed	99.01%	0.6V	2.9kW	69.31KW	28.3ms
P&O	98%	40V	9.3kW	68.6kW	37.8ms
InC	97%	31.7V	7.5kW	67.9kW	35.4ms
MP&O	98.1%	10.2V	4.3kW	68.67kW	38ms

4.2. Dynamic Performance under Varying Irradiance

In this section the Proposed PV MPPT system is simulated in change in irradiance which is shown in Fig 4.5 with total simulation time is 1.5s. The solar irradiance has been changed to $300W/m^2$, $500W/m^2$ and $1000 W/m^2$. From 0s to 0.25s the irradiance remains zero then from 0.25s to 0.5s the irradiance is $300W/m^2$, then from 0.5s to 0.75s the irradiance is $500W/m^2$ and from 0.75s to 1s the irradiance is increased to 1000W/m^2 after the increment the irradiance is decreased to 500W/m^2, from 1s to 1.25s and finally the irradiance is again fall back to zero.

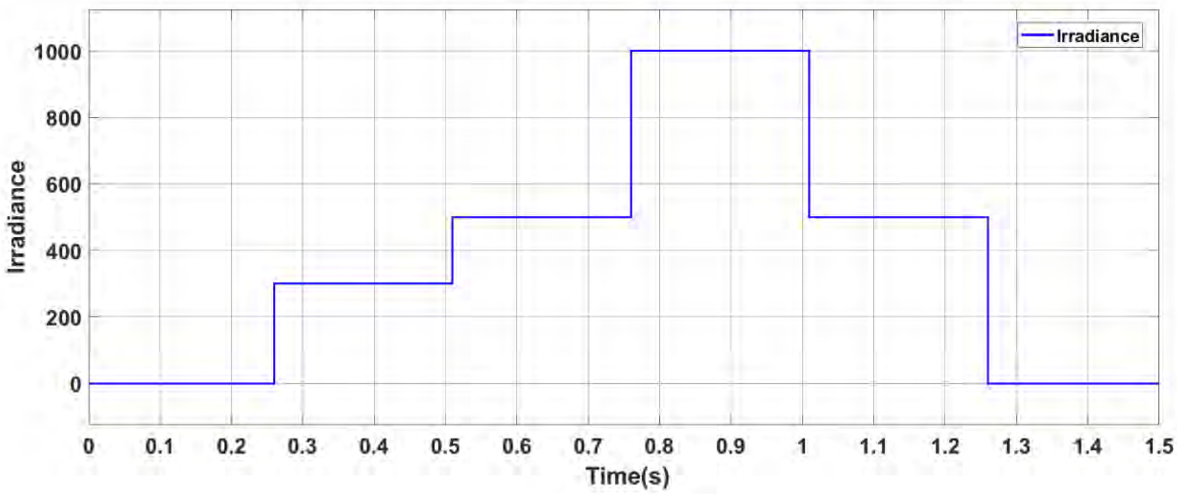

Fig. 4.5. The rapidly changing irradiance.

Figs. 4.6 rigorously confirm the dynamic robustness of the proposed system performs significantly better than the other approaches. The proposed algorithm re-converges to the new MPP in an average of 0.015 seconds after a step change in irradiance, with a little 3% transient power undershoot. On the other hand, the P&O approach has a recognized failure mode, which is a delayed, oscillatory recovery that takes 0.021 seconds to settle and causes a severe undershoot of up to 15%, especially with falling irradiance. With a settling time of 0.02 seconds and a 7% undershoot, the InC technique outperforms the Modified P&O, which improves over standard P&O but is still slower (0.021 seconds) than the suggested method. In comparison to 97.8% for P&O, 98.6% for InC, and 98.3% for Modified P&O, the dynamic tracking efficiency of the suggested technique, which is determined as the energy acquired during the transient relative to the theoretically available energy, surpasses 99.6%. The algorithm's clever mode-switching logic, which differentiates between steady-state operation and transient situations and applies an aggressive, variable-step search only when necessary, is responsible for this higher performance.

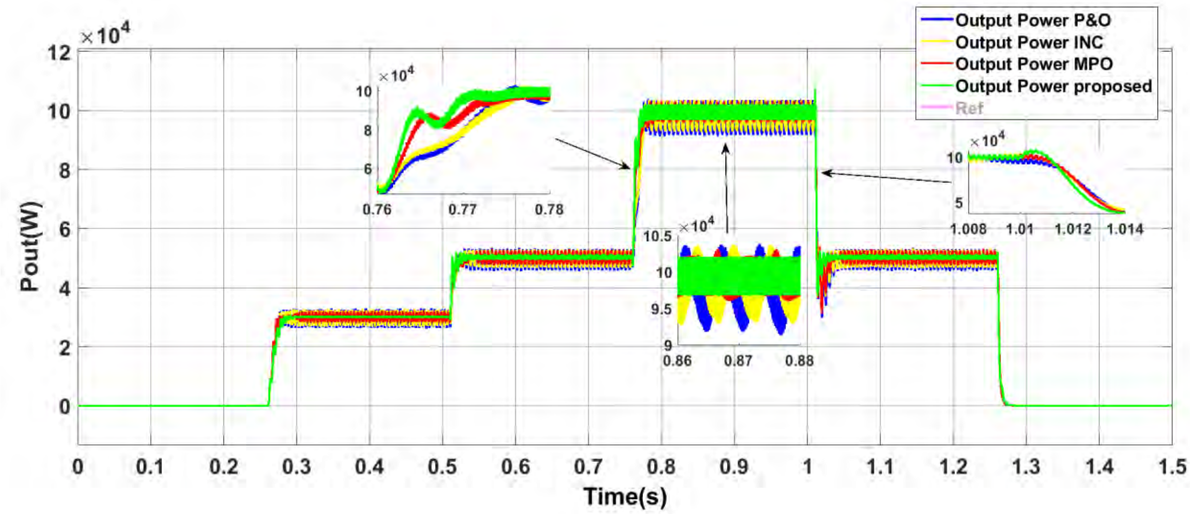

Fig. 4.6. The output power response for dynamic performance with rapidly changes in irradiance.

The steady state convergence speed of the proposed response is given in Fig. 4.7 which is obtained 16.89ms which is a good response compared to the other methods.

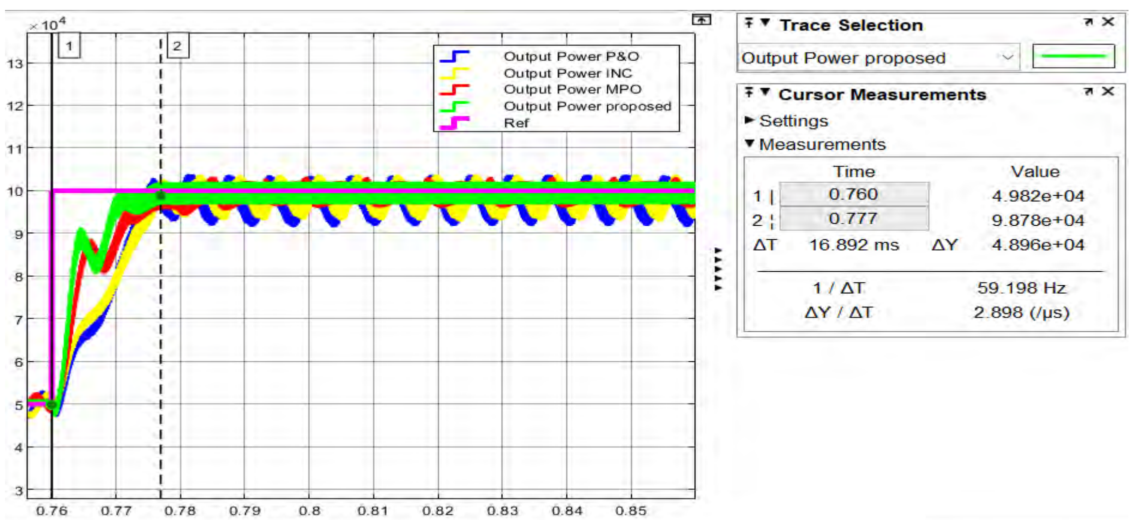

Fig. 4.7. The convergence speed of the proposed system.

Figs. 4.8 and 4.9, which show the duty cycle curve and the resulting PV voltage, respectively, further support the scientific validity of the proposed control technique. The proposed approach eliminates the wasteful continuous perturbation present in P&O-based approaches by producing a steady, non-oscillatory duty cycle in steady state, as shown in Fig. 4.8. While traditional approaches show a staircase of poor changes, its duty cycle adjusts in a single, optimal step during transients. In contrast to voltage oscillations of 20V–36V for the other approaches, this direct and precise control action, shown in Fig. 4.9, produces a fully controlled PV voltage with low ripple (0.7V). In order to improve total system reliability and longevity, stable voltage regulation is crucial because it minimizes stress on PV panels and power electronics, lowers electromagnetic interference, and guarantees compatibility with grid-tie inverters.

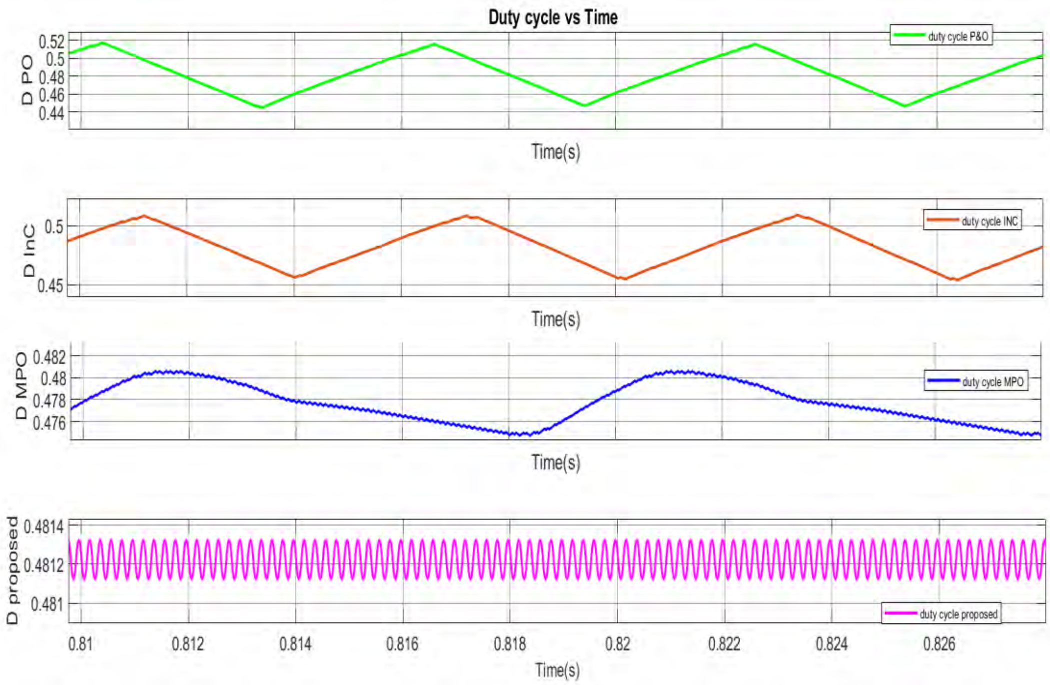

Fig. 4.8. Comparison in changes in duty cycle along with the frequent change in irradiance with 0.01s interval.

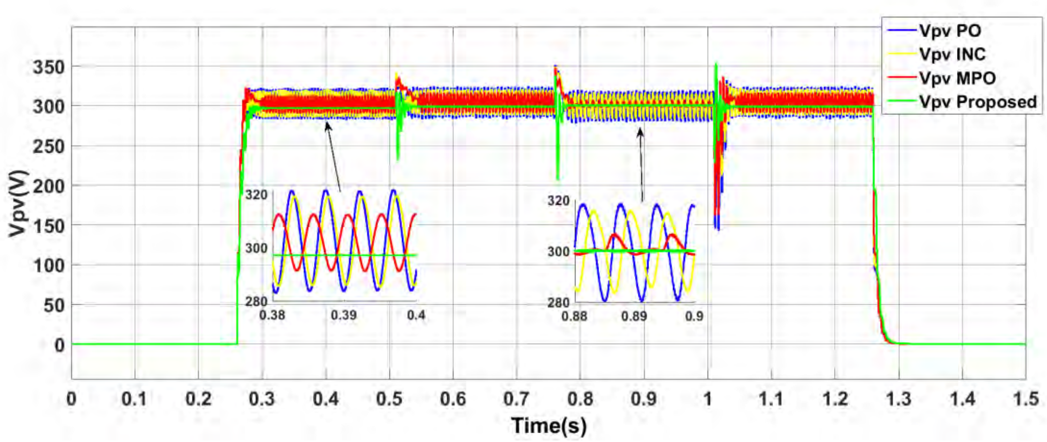

Fig. 4.9. PV voltage waveshapes for different techniques.

Table 4.2 shows the performance detail of all methods. Here for the proposed algorithm the tracking efficiency is obtained 99.6% the convergence speed is 16.8s and voltage oscillation is 0.7V. The obtained values of the performance parameters clearly indicate the better performance of the proposed system.

Table 4.2. Performance analysis for different MPPT methods for dynamic step response

Algorithm	Irradiance	Tracking Efficiency	Voltage Oscillation	Power Oscillation	Output Power	Tracking Speed
Proposed		99.7%	0.2V	0.32kW	29.91kW	38.2ms
P&O		97.1%	38.6V	6.1kW	29.13kW	26.2ms
InC	300W/m^2	96.6%	33.8V	5.2kW	28.98kW	28.6ms
MP&O		96.4%	23.2V	3.2kW	28.92kW	42.1ms
Proposed		99.6%	0.51V	1.5kW	49.8kW	27.9ms
P&O		95%	40.7V	7.3kW	47.5kW	27.8ms
InC	500W/m^2	95.3%	32.8V	6.1kW	47.65kW	27.9ms
MP&O		98.6%	24.8V	5kW	49.3kW	39.3ms
Proposed		99.6%	0.7V	5.2kW	99.6kW	16.8ms
P&O		97.8%	39.1V	12kW	97.8kW	28.8ms
InC	1000W/m^2	98.3%	33.3V	10.9kW	98.3kW	24.6ms
MP&O		98.4%	11.6V	7kW	98.4kW	27.1ms

Since the oscillation is higher for the conventional methods the system parameters are now changed to C_{out} = 1.5uF, C_{in} = 750uF and L = 350uH. Fig 4.10 illustrates the dynamic change in irradiance here the solar irradiance has been changed to 300W/m^2, 500W/m^2, 1000 W/m^2, 800 W/m^2 and 600 W/m^2. From 0s to 0.25s the irradiance remains zero then from 0.25s to 0.5s the irradiance is 300W/m2, then from 0.5s to 0.75s the irradiance is 500W/m2 and from 0.75s to 1s the irradiance is increased to 1000W/m2 after the increment the irradiance is decreased to 800W/m2, from 1s to 1.25s and finally the irradiance is again fall back to 600 W/m^2.

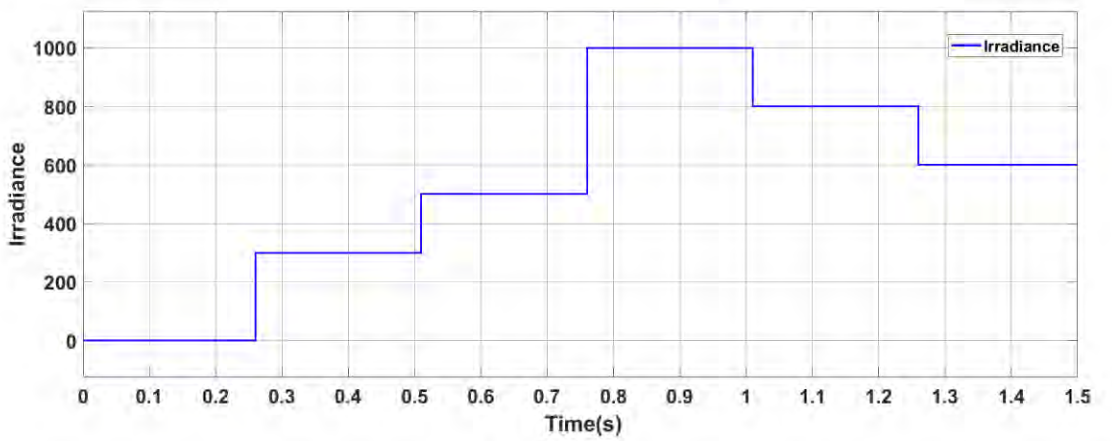

Fig 4.10: The rapidly changing irradiance for new parameters.

Fig 4.11 shows the output power curve response for new parameter values once again the proposed algorithm shows better response than the conventional methods with 99.3% to 99.6% tracking efficiency, in addition the tracking speed also improved from 46.4ms to 21.5ms. The power oscillation is responding better than the conventional methods as it mentioned in detailed in Table 4.3.

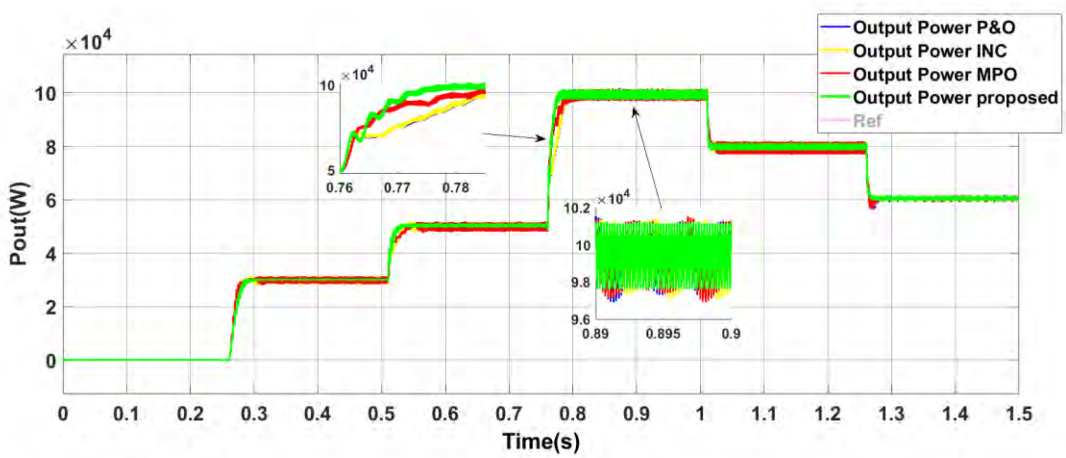

Fig 4.11: The output power response for dynamic performance with rapidly changes in irradiance with new parameter values.

The variation in P_{out}, V_{pv} and duty cycle with the transition of modes are shown in Fig. 4.12, where Mode 0 is selected when the irradiance is 500W/m2 and Mode 1 is selected for 100W/m2 irradiance. Other than mentioned irradiance values both Mode 0 and Mode 1 occurs, where Mode 0 is selected at the starting stage and when the duty cycle is adjusted Mode 1 occurs.

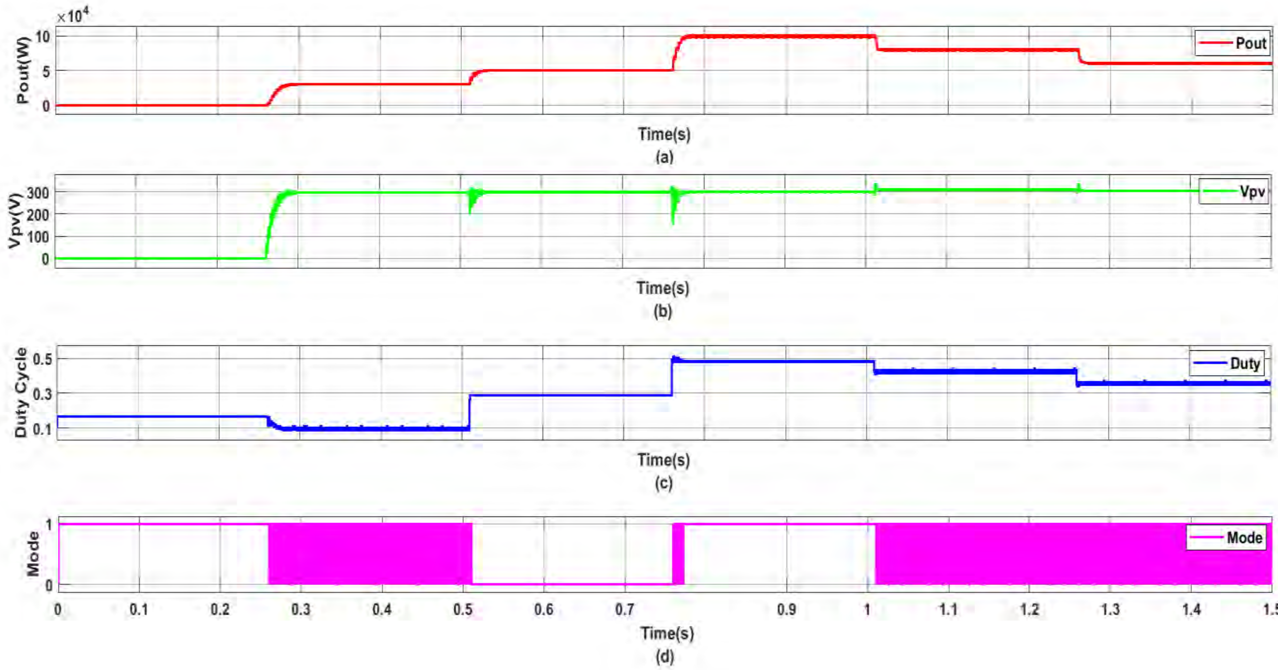

Fig. 4.12. Change in P_{out}, V_{pv} and Duty Cycle with Mode Transition for dynamic irradiance with new parameter values

Figs. 4.13 and Fig. 4.14, show the duty cycle curve and the resulting PV voltage, respectively, further support the scientific validity of the proposed control technique. The proposed approach eliminates the wasteful continuous perturbation present in P&O-based approaches by producing a steady, non-oscillatory duty cycle in steady state, as shown in Fig. 4.13. While traditional approaches show a staircase of poor changes, its duty cycle adjusts in a single, optimal step during transients. In contrast to voltage oscillations of 14V–16V for the other approaches, this direct and precise control action, shown in Fig. 4.14, produces a fully controlled PV voltage with low ripple (3V).

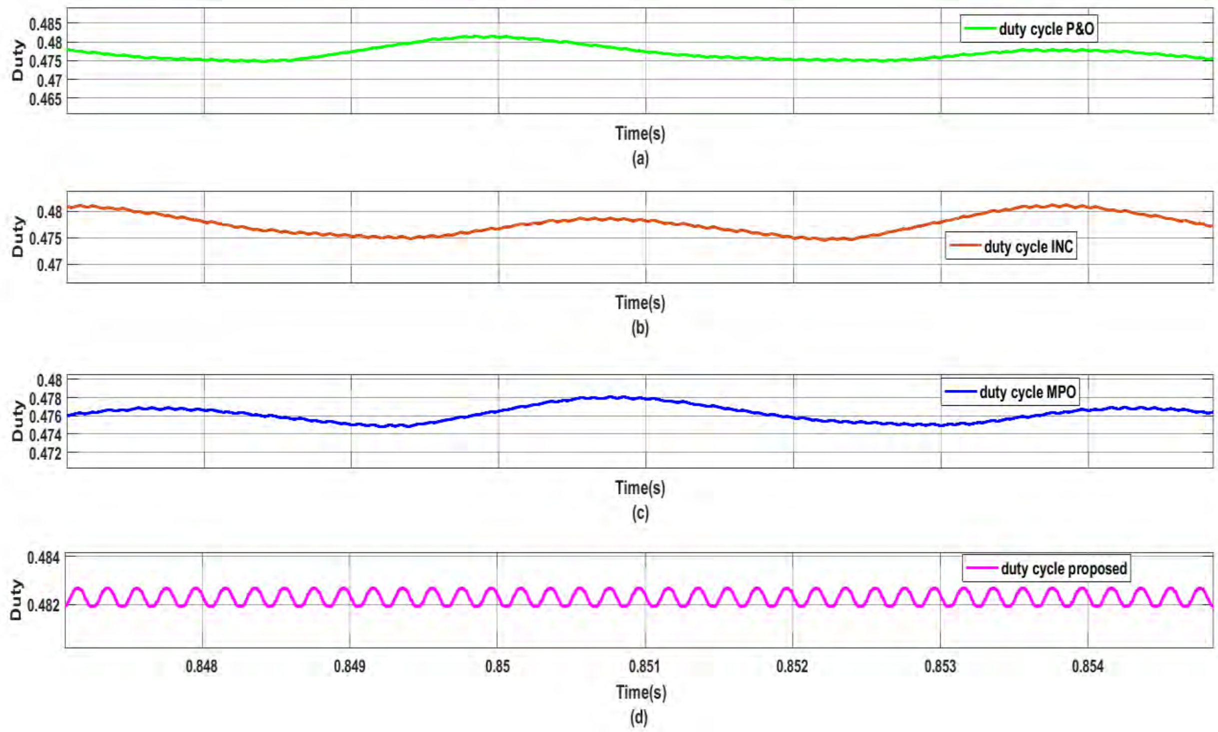

Fig. 4.13. Comparison in changes in duty cycle along with the frequent change in irradiance with 0.01s interval with new parameter values.

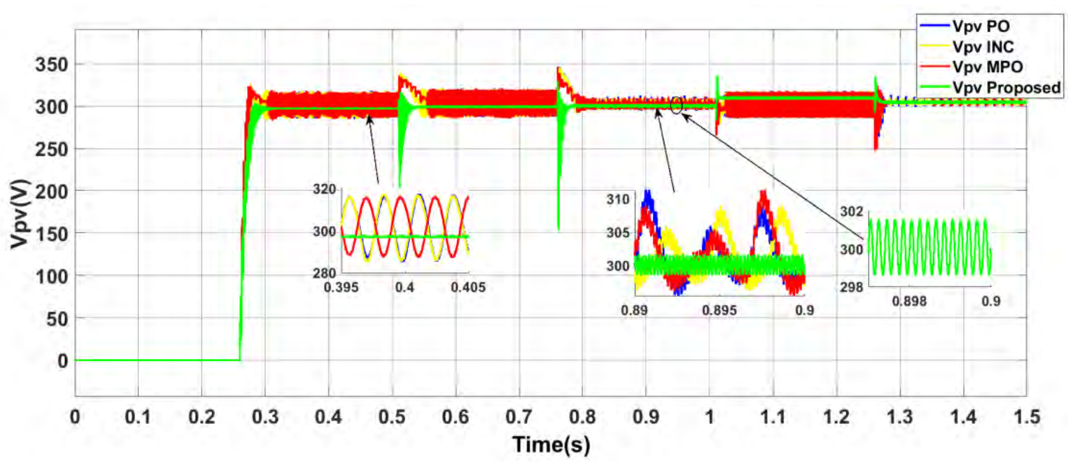

Fig. 4.14. PV voltage waveshapes for different techniques with new parameter values.

Table 4.3 shows the suggested approach regularly outperforms the others in tracking efficiency, achieving the highest values (99.7% at 300 W/m², 99.6% at 500 W/m², and 99.6% at 1000 W/m²). More importantly, it performs exceptionally well in terms of stability, showing far less power oscillation (0.21–3.6 kW) and voltage oscillation (0.5V–2.9V) than the other algorithms, which exhibit oscillations an order of magnitude bigger (e.g., 13.9–33.2V and 2.75–4.5 kW). This suggests a power output that is significantly smoother and more dependable. Additionally, the suggested approach has the fastest tracking speed at all irradiance levels (46.4 ms, 26.6 ms, and 21.5 ms), which enables it to adjust to changing environmental conditions faster.

Table 4.3. Performance analysis for different MPPT methods for dynamic step response with new parameter values

Algorithm	Irradiance	Tracking Efficiency	Voltage Oscillation	Power Oscillation	Output Power	Tracking Speed
Proposed		99.3%	0.5V	0.21 kW	29.8kW	46.4ms
P&O		98.5%	31.8V	2.8 kW	29.55kW	48.9ms
InC	300W/m^2	98.6%	31.6V	2.75 kW	29.58kW	48.8ms
MP&O		98.3%	31.8V	2.75 kW	29.49kW	47.3ms
Proposed		99.6%	1.6V	1kW	49.8kW	26.6ms
P&O		99.2%	32.6V	3.4kW	49.6kW	37.2ms
InC	500W/m^2	99.2%	33.1V	3.4kW	49.6kW	37.1ms
MP&O		99.3%	33.2V	3.5kW	49.65kW	51ms
Proposed		99.6%	2.9V	3.6kW	99.6kW	21.5ms
P&O		99.4%	16.5V	4.5kW	99.4kW	34.9ms
InC	1000W/m^2	99.4%	13.9V	4.4kW	99.4kW	34.7ms
MP&O		99.5%	16.5V	4.4kW	99.5kW	30.1ms

The 24 hours practical irradiance data for Dhaka city is given is Fig. 4.15 and the output power response curve is given in Fig. 4.16, where it is clearly seen that the power oscillation for the proposed algorithm shows better response than the conventional methods. Although another observation is during the starting period the conventional methods works better than the proposed algorithm. It can be observed that the tracking speed is performing less than the conventional methods when the irradiance value is less than 250W/m^2.

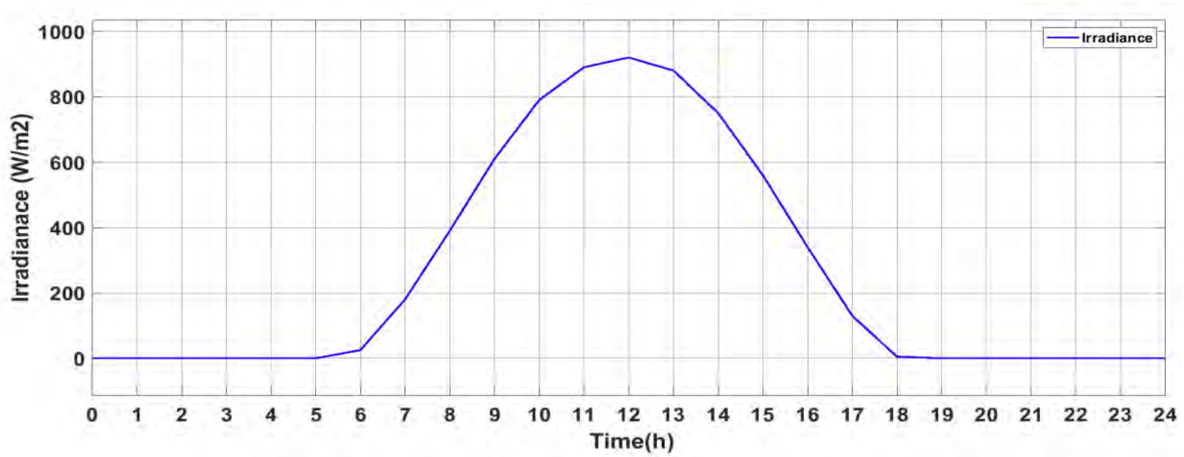

Fig. 4.15. Practical irradiance profile of Dhaka city for 24 hours.

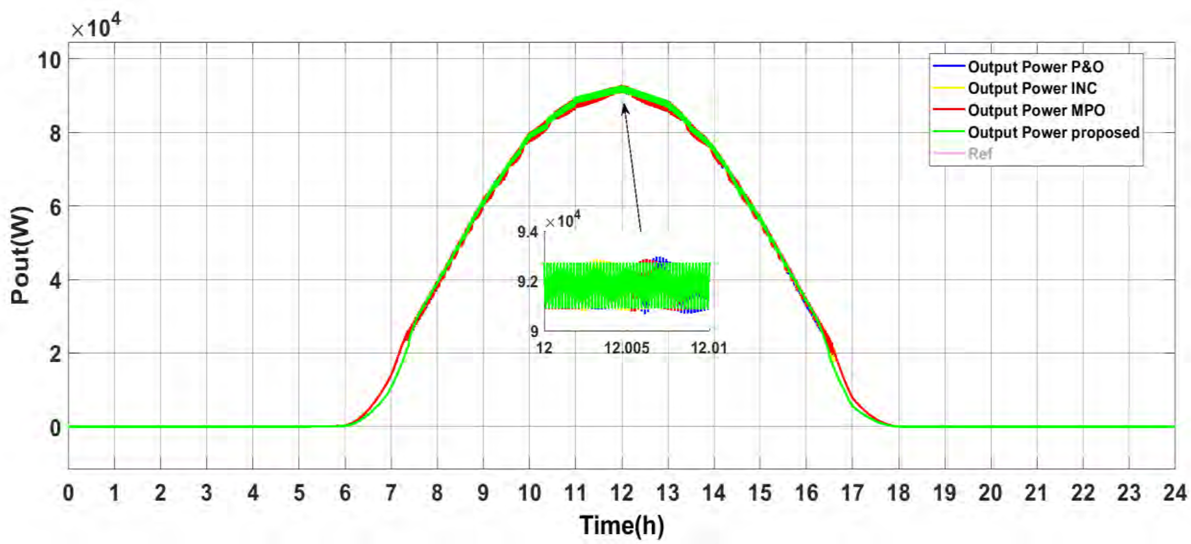

Fig. 4.16. Output power response for 24 hours

Variation in P_{out}, V_{pv} and Duty Cycle curve with Mode transition for 24 hours change in irradiance is shown in Fig. 4.17, where it can be clearly observed that Mode 0 is selected when the irradiance is between 8 to 9-hour. During the peak time at 11 to 13-hour Mode 1 is selected. The change in duty cycle curve is showing in Fig. 4.18 where it can be seen that the duty for the proposed method shows spike when Mode 0 occurs, since step size is added with the duty cycle in order to sense the proper voltage.

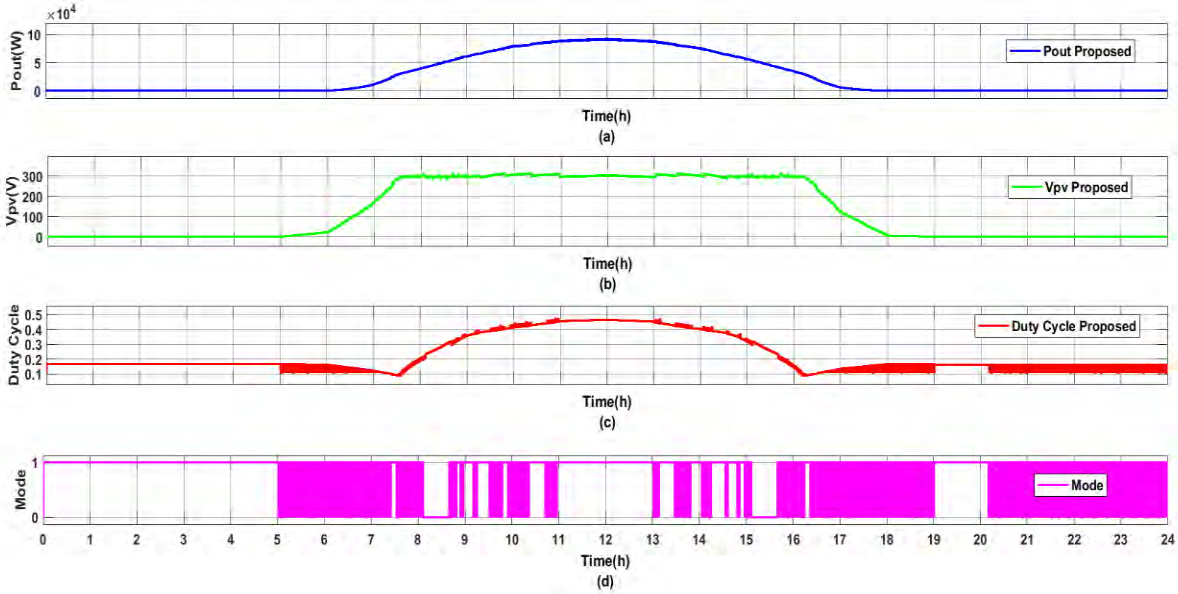

Fig 4.17. Variation in P_{out}, V_{pv} and Duty Cycle with Mode Transition for 24 hours change in irradiance

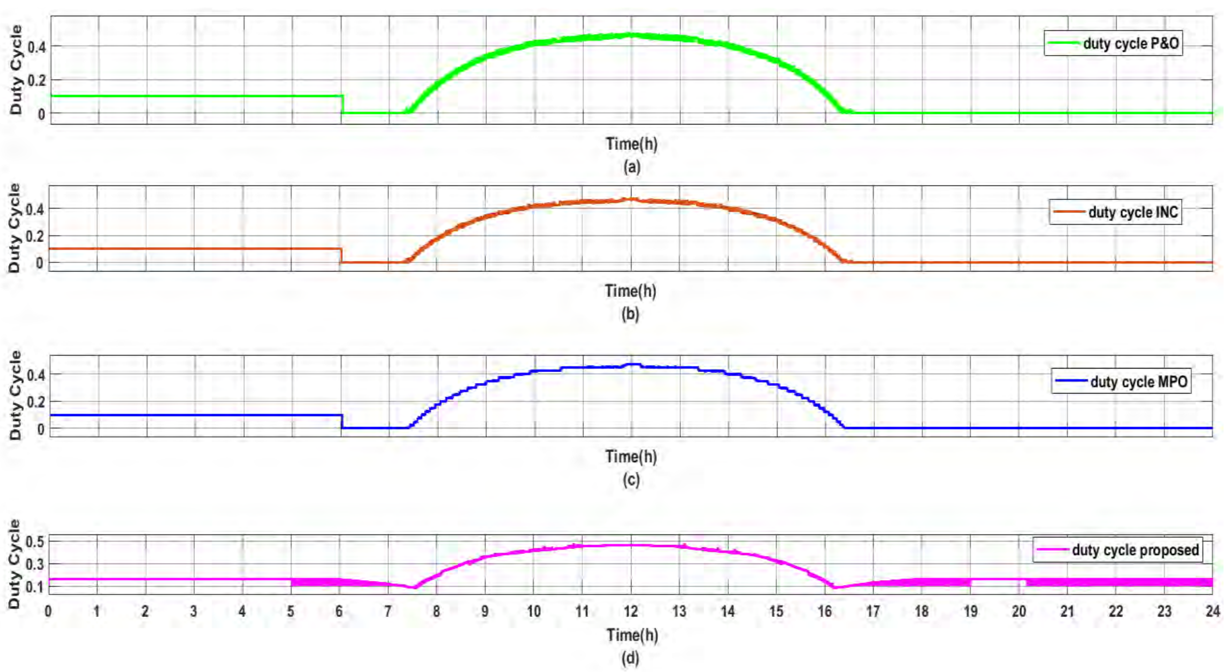

Fig 4.18. Change of duty cycle for 24 hours.

The findings of the proposed method is compared with the published articles in Table 4.4 where the tracking efficiency and tracking speed compared, moreover the control variable, algorithm complexity and converter type is compared as well.

Table 4.4. Comparison between the proposed algorithms with the published works

Ref	Algorithm	Control Variable	Complexity	Converter Type	Tracking Efficiency (%)	Tracking Speed (ms)
[1]	Enhanced P&O	Voltage	Low	Boost	99.8	15.8
[122]	Modified P&O	Voltage	Low	Boost	99.8	50
[123]	ANN-GT ANN-TI	Voltage	Moderate	Boost	98.25 98.16	1500 1300
[124]	TB-MPPT	Duty cycle	Low	Modified Boost	94.2	Not Mentioned
[125]	IC	Duty cycle	Low	Boost	95	81
[126]	ABC	Voltage	High	Boost	98.92	160
[127]	ANN	Voltage	High	Boost	98.25	140
	IBA – FLC	Voltage	High	Boost	99.23	110
[128]	HWO – PS	Voltage	High	VSI	98.30	130
[129]	MRAC	Voltage	Moderate	Boost	99.6	4
	WOA	Voltage	High	Boost	98.92	28
[130]	GWO	Voltage	High	Boost	99.50	17.5
	PSO	Voltage	High	Boost	98.10	27
This Article	Sweep assisted enhanced adaptive Fuzzy-P&O	Voltage	Moderate	Boost	99.6	16.8

4.3. Detailed analysis of 100kW Proposed PV MPPT System

The simulated steady-state PV data (irradiance, duty cycle, voltage, and current) has been set smooth interpolated curves to analyze the relationship between irradiance and system performance. First, it defines the raw measured data, then generates a fine-grained irradiance range (300–1000 W/m²) and applied piecewise cubic Hermite interpolation (PCHIP) to obtain smooth profiles of duty cycle, PV voltage, and current. Using these, it computes the output power as P=Vpv×Ipv.

Duty cycle vs irradiance showing how the control duty increases with irradiance in Fig. 4.19. Power vs irradiance curve in Fig. 4.20 highlights the nearly linear rise of power with irradiance, 3D scatter plot relating irradiance, duty, and power in one space is given in Fig. 4.21. Interpolated 3D surface plot using scattered data interpolation in Fig. 4.22 creates a smooth continuous surface of power versus irradiance and duty.

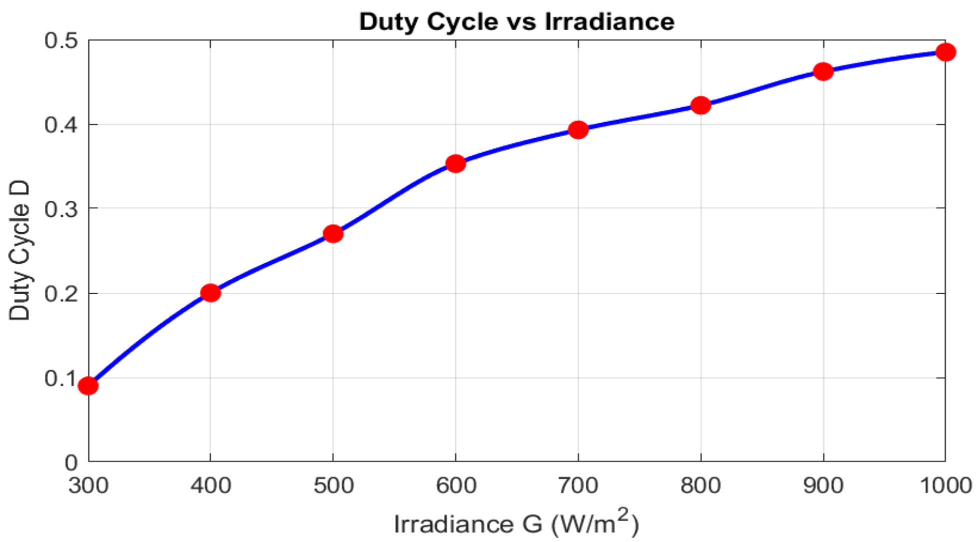

Fig. 4.19. Duty cycle vs Irradiance plot.

Fig. 4.20. Output Power vs Irradiance plot.

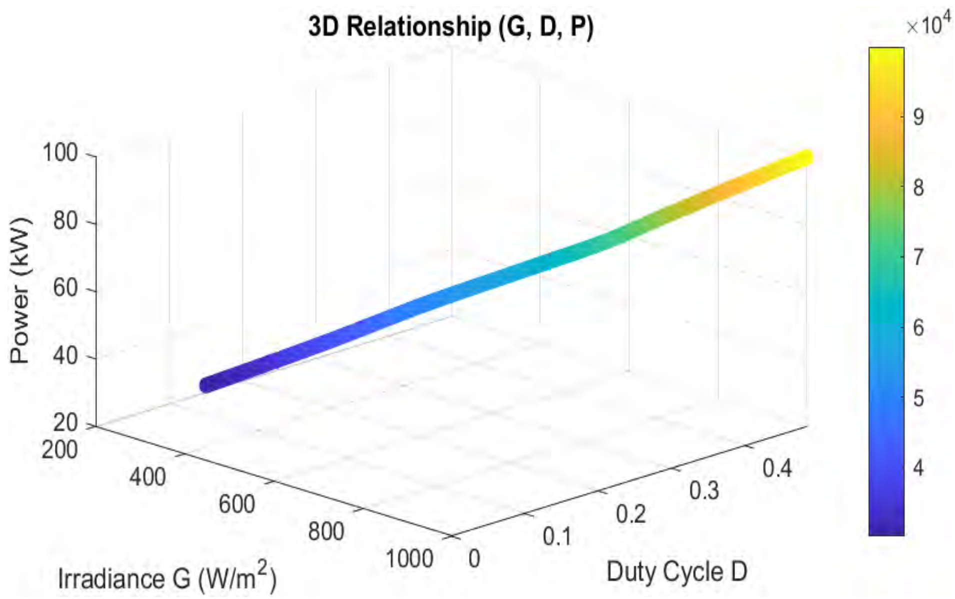

Fig. 4.21. 3D relationship between Irradiance, Duty Cycle and Power (kW)

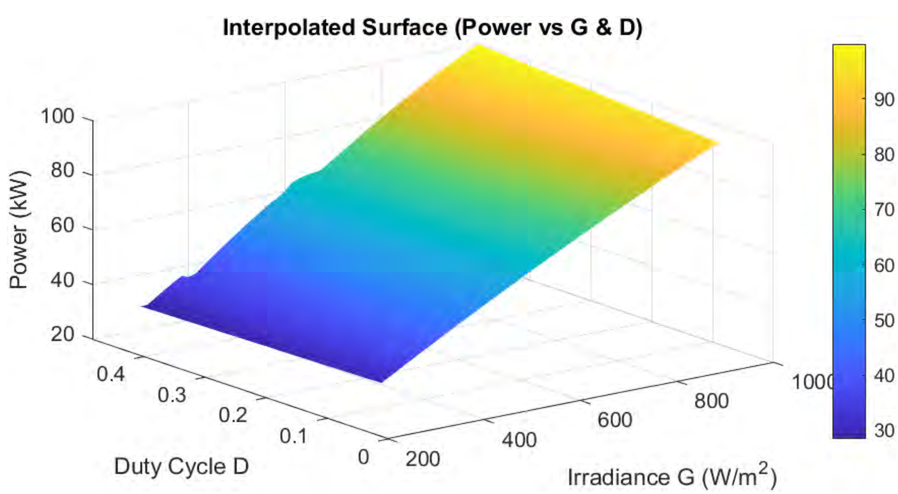

Fig. 4.22. Interpolated surface plot for Irradiance, Duty Cycle and Power (kW)

Fig. 4.23 to Fig. 4.25 shows the how PV voltage current and power changes with the variations of duty cycle. The voltage vs Duty cycle plot is given in Fig. 4.23 the duty cycle has been varied from 0.05 to 0.5, here at 0.09 the voltage is obtained 297V which is the MPP voltage for 300W/m^2, likewise the maximum voltage is obtained close to 301V which is the MPP voltage for 1000W/m^2 the corresponding duty cycle is 0.485.

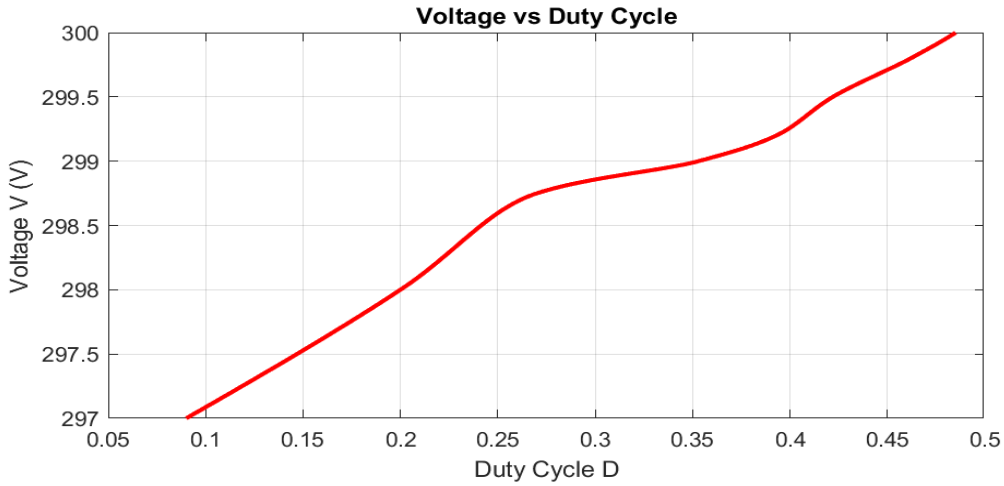

Fig. 4.23. Voltage vs duty cycle plot.

The current vs Duty cycle plot is given in Fig. 4.24 the duty cycle has been varied from 0.05 to 0.5, here at 0.09 the current is obtained around 101 A which is the MPP current for 300W/m^2, likewise the maximum current is obtained close to 333A which is the MPP current for 1000W/m^2 the corresponding duty cycle is 0.485.

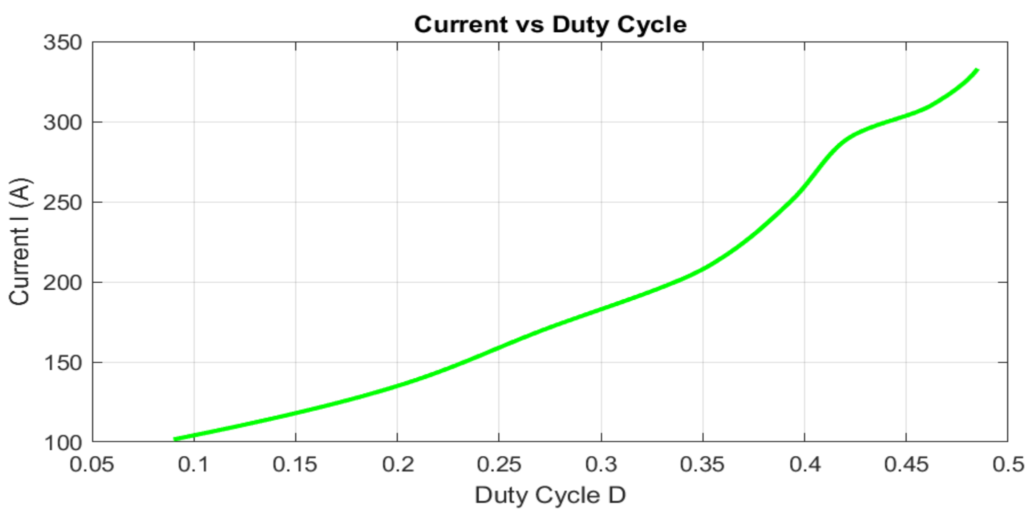

Fig. 4.24. Current vs duty cycle plot.

The Output power vs Duty cycle plot is given in Fig. 4.25 the duty cycle has been varied from 0.05 to 0.5, here at 0.09 the current is obtained around 30kW which is the maximum power for

$300W/m^2$, likewise the maximum power is obtained close to 100kW which is the Power for $1000W/m^2$ the corresponding duty cycle is 0.485.

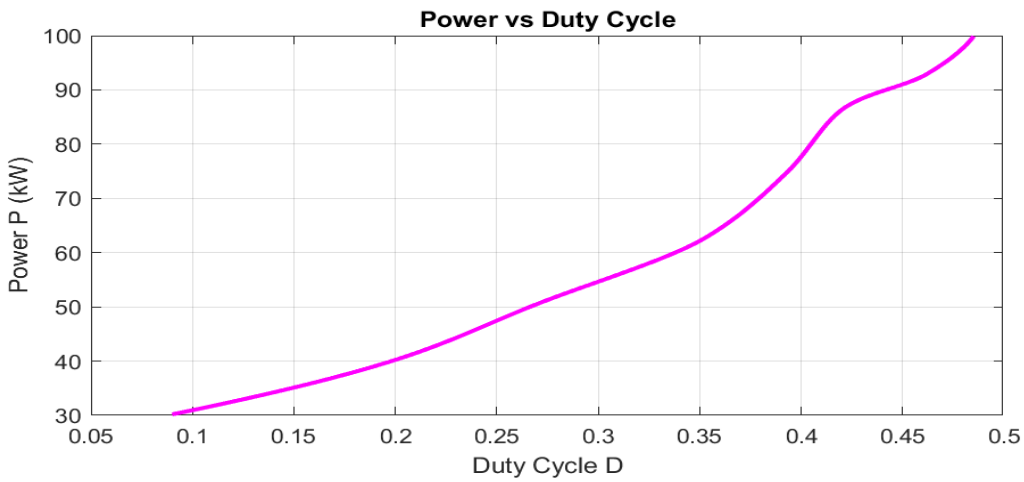

Fig. 4.25. Current vs duty cycle plot.

The simulation of a 100 kW PV plant is more than just a scalability test; it is an essential illustration of the usefulness and industrial applicability of the suggested approach. These large-scale findings have two implications. First, they demonstrate that the superior tracking speed, less oscillation, and high efficiency shown at the module level transfer linearly and effectively to a full-scale power plant. For a 100 kW system, the energy improvements of 1-3% might appear insignificant for a single panel, but they add up to thousands of extra kilowatt-hours produced yearly, which is a significant financial benefit. Second, the algorithm's stability and compliance with real-world power electronics in a high-power setting where problems like converter switching noise, system inertia, and greater parasitic capacitances can destabilize less robust controllers are confirmed by large-scale simulation. The algorithm's readiness for commercial deployment is strongly supported by demonstrating consistent, superior control on a 100 kW plant, transforming the contribution from a theoretical advancement to a solution with immediate practical and economic benefit.

Chapter 5

Conclusion and Future Work

5.1. Summary of Findings

In this thesis, a sweep assisted Hybrid Enhanced Adaptive Fuzzy P&O MPPT algorithm for a 100 kW photovoltaic boost converter was designed and evaluated.

- In order to improve stability, the suggested method merged an adaptive fuzzy perturb and observe (P&O) technique with a sweep-based initialization mode, adding voltage thresholds (v1, v2).
- Under changing irradiance and temperature circumstances, the hybrid method showed the capacity to decrease steady-state oscillations, increase convergence speed, and preserve tracking accuracy.
- The overall tracking efficiency for the system is obtained 99.6%, the tracking speed is 16.8 ms and the voltage oscillation is about 0.7%.
- According to MATLAB/Simulink simulation findings, the controller continuously modified the operating point close to the maximum power point (MPP), attaining greater efficiency than standalone fuzzy-based techniques and traditional P&O.
- The algorithm exhibited robustness during partial shading and dynamic transients, where it successfully avoided local maxima and reinitiated sweep mode when necessary.

5.2. Contributions to the Field

The following significant results demonstrate how the research advances the field of renewable energy conversion and control:

- Hybrid MPPT Framework: A dual-mode controller that uses fuzzy-enhanced P&O for fine-tuning steady-state control and sweep-based exploration for precise initialization is introduced.
- Adaptive Voltage Thresholding: minimizes divergence and ensures bounded reference voltage by integrating dynamic constraints (v1 and v2) scaled with the estimated Vmpp.

- Robust Fuzzy Inference System: Adaptive adjustment of the reference voltage increment (ΔVref) is made possible by the creation of a 25-rule fuzzy decision matrix that is specific to PV dynamics.
- Performance Improvement in PV Systems: Excellent steady-state and transient tracking efficiency is demonstrated, indicating possibilities for large-scale PV installations where energy yield and dependability are crucial.
- Scalable Control Design: An approach that can be modified to accommodate varying array sizes and converter ratings without requiring significant changes to the algorithmic framework.

5.3. Limitations of the Research

A limitation of this research is the proposed algorithm is not simulated in partial shading conditions as a result complete system response is not yet observed. Moreover the proposed algorithm is responding slowly below 200W/m^2 which leads a drawback at lower irradiance values.

5.4. Recommendations for Future Work

Although the suggested hybrid algorithm saw significant gains, a few additions could increase its usefulness even more:

- Hardware Implementation: Real-time validation on a controller based on DSP or FPGA to assess realistic performance, including control delays, switching losses, and sensor noise.
- Artificial Intelligence Integration: To allow self-tuning in extremely nonlinear circumstances, the fuzzy P&O scheme is coupled with machine learning methods as adaptive neuro-fuzzy inference systems (ANFIS) or artificial neural networks (ANN).
- Multi-Objective Optimization: Using the same MPPT architecture to incorporate grid-support features like fault ride-through, reactive power adjustment, and harmonic minimization.

References

[1] Ali, A.I.M., Mousa, H.H., Mohamed, H.R.A., Kamel, S., Hassan, A.S., Alaas, Z.M., Mohamed, E.E. and Abdallah, A.R.Y., 2023. An enhanced P&O MPPT algorithm with concise search area for grid-tied PV systems. IEEE Access, 11, pp.79408-79421.

[2] Ali, A.I., Sayed, M.A. and Mohamed, E.E., 2018. Modified efficient perturb and observe maximum power point tracking technique for grid-tied PV system. International Journal of Electrical Power & Energy Systems, 99, pp.192-202.

[3] J. Ahmed and Z. Salam, ''An improved perturb and observe (P&O) maximum power point tracking (MPPT) algorithm for higher efficiency,'' *Appl. Energy*, vol. 150, pp. 97–108, Jul. 2015.

[4] H. H. H. Mousa, A.-R. Youssef, I. Hamdan, M. Ahamed, and E. E. M. Mohamed, ''Performance assessment of robust P&O algorithm using optimal hypothetical position of generator speed,'' *IEEE Access*, vol. 9, pp. 30469–30485, 2021.

[5] N. Femia, G. Petrone, G. Spagnuolo, and M. Vitelli, ''A technique for improving P&O MPPT performances of double-stage grid-connected photovoltaic systems,'' *IEEE Trans. Ind. Electron.*, vol. 56, no. 11, pp. 4473–4482, Nov. 2009.

[6] A. I. M. Ali, M. Abdallah, T. Takeshita, and Z. M. Alaas, ''Three-phase single-carrier PWM inverter for isolated grid-tied PV applications,'' IEEE Access, vol. 10, pp. 93395–93411, 2022.

[7] Piegari, L. and Rizzo, R., 2010. Adaptive perturb and observe algorithm for photovoltaic maximum power point tracking. IET Renewable Power Generation, 4(4), pp.317-328.

[8] I. Rezwana, A. Botros, A. Attieh, S. I. Ocean and E. Hossain, "Assessing the Impact of Extreme Weather Conditions on Solar Module Performance: A Comprehensive Hardware Evaluation," 2024 IEEE Power & Energy Society General Meeting (PESGM), Seattle, WA, USA, 2024, pp. 1-5, doi: 10.1109/PESGM51994.2024.10761096.

[9] M. H. Rashid, *Power Electronics Handbook*, 5th ed. Butterworth-Heinemann, 2023.

[10] Hohm, D.P. and Ropp, M.E., 2000, September. Comparative study of maximum power point tracking algorithms using an experimental, programmable, maximum power point tracking test bed. In Conference record of the twenty-eighth IEEE photovoltaic specialists conference-2000 (Cat. No. 00CH37036) (pp. 1699-1702). IEEE.

[11] Femia, N., Petrone, G., Spagnuolo, G. and Vitelli, M., 2005. Optimization of perturb and observe maximum power point tracking method. IEEE transactions on power electronics, 20(4), pp.963-973.

[12] Abdelsalam, A.K., Massoud, A.M., Ahmed, S. and Enjeti, P.N., 2011. High-performance adaptive perturb and observe MPPT technique for photovoltaic-based microgrids. IEEE Transactions on power electronics, 26(4), pp.1010-1021.

[13] Zhang, F., Thanapalan, K., Procter, A., Carr, S. and Maddy, J., 2013. Adaptive hybrid maximum power point tracking method for a photovoltaic system. IEEE Transactions on Energy Conversion, 28(2), pp.353-360.

[14] Yang, Y. and Zhao, F.P., 2011. Adaptive perturb and observe MPPT technique for grid-connected photovoltaic inverters. Procedia Engineering, 23, pp.468-473.

[15] Kamran, M., Mudassar, M., Fazal, M.R., Asghar, M.U., Bilal, M. and Asghar, R., 2020. Implementation of improved Perturb & Observe MPPT technique with confined search space for standalone photovoltaic system. Journal of King Saud University-Engineering Sciences, 32(7), pp.432-441.

[16] Noh, H.J., Lee, D.Y. and Hyun, D.S., 2002, November. An improved MPPT converter with current compensation method for small scaled PV-applications. In IEEE 2002 28th Annual Conference of the Industrial Electronics Society. IECON 02 (Vol. 2, pp. 1113-1118). IEEE.

[17] Masoum, M.A., Dehbonei, H. and Fuchs, E.F., 2003. Theoretical and experimental analyses of photovoltaic systems with voltageand current-based maximum power-point tracking. IEEE Transactions on energy conversion, 17(4), pp.514-522.

[18] Hart, G.W., Branz, H.M. and Cox Iii, C.H., 1984. Experimental tests of open-loop maximum-power-point tracking techniques for photovoltaic arrays. Solar cells, 13(2), pp.185-195.

[19] Marques Lameirinhas, R.A.; Torres, J.P.N.; de Melo Cunha, J.P. A Photovoltaic Technology Review: History, Fundamentals and Applications. Energies 2022, 15, 1823. https://doi.org/10.3390/en15051823

[20] Al-Majidi, S.D.A., 2020. Efficient Maximum Power Point Tracking Techniques for a Grid-connected Photovoltaic System using Artificial Intelligence (Doctoral dissertation, Brunel University London).

[21] Chen, Y., Chen, D., Altermatt, P.P., Zhang, S., Wang, L., Zhang, X., Xu, J., Feng, Z., Shen, H. and Verlinden, P.J., 2023. Technology evolution of the photovoltaic industry: learning from history and recent progress. Progress in Photovoltaics: Research and Applications, 31(12), pp.1194-1204.

[22] Tyagi, V.V., Rahim, N.A. and Rahim, N.A., 2013. Progress in solar PV technology: Research and achievement. Renewable and sustainable energy reviews, 20, pp.443-461.

[23] Verbong, G., Geels, F.W. and Raven, R., 2013. Multi-niche analysis of dynamics and policies in Dutch renewable energy innovation journeys (1970-2006): hype-cycles, closed networks and

technology-focused learning. In The dynamics of sustainable innovation journeys (pp. 35-53). Routledge.

[24] Obeidat, F., 2018. A comprehensive review of future photovoltaic systems. Solar Energy, 163, pp.545-551.

[25] Sahu, B.K., 2015. A study on global solar PV energy developments and policies with special focus on the top ten solar PV power producing countries. Renewable and Sustainable Energy Reviews, 43, pp.621-634.

[26] Obeidat, F., 2018. A comprehensive review of future photovoltaic systems. Solar Energy, 163, pp.545-551.

[27] Grau, T., Huo, M. and Neuhoff, K., 2012. Survey of photovoltaic industry and policy in Germany and China. Energy policy, 51, pp.20-37.

[28] Van den Heuvel, S.T. and Van den Bergh, J.C., 2009. Multilevel assessment of diversity, innovation and selection in the solar photovoltaic industry. Structural Change and Economic Dynamics, 20(1), pp.50-60.

[29] Tian, W., Wang, Y., Ren, J. and Zhu, L., 2007. Effect of urban climate on building integrated photovoltaics performance. Energy conversion and management, 48(1), pp.1-8.

[30] Hara, K., Horiguchi, T., Kinoshita, T., Sayama, K., Sugihara, H. and Arakawa, H., 2000. Highly efficient photon-to-electron conversion with mercurochrome-sensitized nanoporous oxide semiconductor solar cells. Solar energy materials and solar cells, 64(2), pp.115-134.

[31] Tan, Y.T., Kirschen, D.S. and Jenkins, N., 2004. A model of PV generation suitable for stability analysis. IEEE Transactions on energy conversion, 19(4), pp.748-755.

[32] Ishaque, K. and Salam, Z., 2012. A deterministic particle swarm optimization maximum power point tracker for photovoltaic system under partial shading condition. IEEE transactions on industrial electronics, 60(8), pp.3195-3206.

[33] Ram, J.P., Babu, T.S. and Rajasekar, N., 2017. A comprehensive review on solar PV maximum power point tracking techniques. Renewable and Sustainable Energy Reviews, 67, pp.826-847.

[34] Al-Majidi, S.D., Abbod, M.F. and Al-Raweshidy, H.S., 2018. A novel maximum power point tracking technique based on fuzzy logic for photovoltaic systems. International Journal of Hydrogen Energy, 43(31), pp.14158-14171.

[35] Orioli, A. and Di Gangi, A., 2013. Load mismatch of grid-connected photovoltaic systems: Review of the effects and analysis in an urban context. Renewable and Sustainable Energy Reviews, 21, pp.13-28.

[36] Haillant, O., 2011. Accelerated weathering testing principles to estimate the service life of organic PV modules. Solar Energy Materials and Solar Cells, 95(5), pp.1284-1292.

[37] Branker, K., Pathak, M.J.M. and Pearce, J.M., 2011. A review of solar photovoltaic levelized cost of electricity. Renewable and sustainable energy reviews, 15(9), pp.4470-4482.

[38] Saravanan, S. and Babu, N.R., 2016. Maximum power point tracking algorithms for photovoltaic system–A review. Renewable and sustainable energy reviews, 57, pp.192-204.

[39] Farzaneh, J., Keypour, R. and Karsaz, A., 2019. A novel fast maximum power point tracking for a PV system using hybrid PSO-ANFIS algorithm under partial shading conditions. International Journal of Industrial Electronics Control and Optimization, 2(1), pp.47-58.

[40] Patcharaprakiti, N., Premrudeepreechacharn, S. and Sriuthaisiriwong, Y., 2005. Maximum power point tracking using adaptive fuzzy logic control for grid-connected photovoltaic system. Renewable energy, 30(11), pp.1771-1788.

[41] Birane, M., Larbes, C. and Cheknane, A., 2017. Comparative study and performance evaluation of central and distributed topologies of photovoltaic system. International journal of hydrogen energy, 42(13), pp.8703-8711.

[42] Faranda, R. and Leva, S., 2008. Energy comparison of MPPT techniques for PV Systems. WSEAS transactions on power systems, 3(6), pp.446-455.

[43] Al-Majidi, S.D., Abbod, M.F. and Al-Raweshidy, H.S., 2019, September. Design of an intelligent MPPT based on ANN using a real photovoltaic system data. In 2019 54th International universities power engineering conference (UPEC) (pp. 1-6). IEEE.

[44] Elgendy, M.A., Zahawi, B. and Atkinson, D.J., 2012. Assessment of the incremental conductance maximum power point tracking algorithm. IEEE Transactions on sustainable energy, 4(1), pp.108-117.

[45] Bhukya, L. and Nandiraju, S., 2020. A novel photovoltaic maximum power point tracking technique based on grasshopper optimized fuzzy logic approach. International journal of hydrogen energy, 45(16), pp.9416-9427.

[46] Duman, S., Yorukeren, N. and Altas, I.H., 2018. A novel MPPT algorithm based on optimized artificial neural network by using FPSOGSA for standalone photovoltaic energy systems. Neural Computing and Applications, 29(1), pp.257-278.

[47] Al-Majidi, S.D., Abbod, M.F. and Al-Raweshidy, H.S., 2018, September. A modified P&O-MPPT based on Pythagorean Theorem and CV-MPPT for PV Systems. In 2018 53rd International Universities Power Engineering Conference (UPEC) (pp. 1-6). IEEE.

[48] D'Souza, N.S., Lopes, L.A. and Liu, X., 2010. Comparative study of variable size perturbation and observation maximum power point trackers for PV systems. Electric Power Systems Research, 80(3), pp.296-305.

[49] Kermadi, M. and Berkouk, E.M., 2017. Artificial intelligence-based maximum power point tracking controllers for Photovoltaic systems: Comparative study. Renewable and Sustainable Energy Reviews, 69, pp.369-386.

[50] Salah, C.B. and Ouali, M., 2011. Comparison of fuzzy logic and neural network in maximum power point tracker for PV systems. Electric Power Systems Research, 81(1), pp.43-50.

[51] Subudhi, B. and Pradhan, R., 2012. A comparative study on maximum power point tracking techniques for photovoltaic power systems. IEEE transactions on Sustainable Energy, 4(1), pp.89-98.

[52] Bollipo, R.B., Mikkili, S. and Bonthagorla, P.K., 2020. Hybrid, optimal, intelligent and classical PV MPPT techniques: A review. CSEE Journal of Power and Energy Systems, 7(1), pp.9-33.

[53] Masoum, M.A., Dehbonei, H. and Fuchs, E.F., 2003. Theoretical and experimental analyses of photovoltaic systems with voltageand current-based maximum power-point tracking. IEEE Transactions on energy conversion, 17(4), pp.514-522.

[54] Ahmad, R., Murtaza, A.F. and Sher, H.A., 2019. Power tracking techniques for efficient operation of photovoltaic array in solar applications–A review. Renewable and Sustainable Energy Reviews, 101, pp.82-102.

[55] De Brito, M.A.G., Galotto, L., Sampaio, L.P., e Melo, G.D.A. and Canesin, C.A., 2012. Evaluation of the main MPPT techniques for photovoltaic applications. IEEE transactions on industrial electronics, 60(3), pp.1156-1167.

[56] Seyedmahmoudian, M., Horan, B., Soon, T.K., Rahmani, R., Oo, A.M.T., Mekhilef, S. and Stojcevski, A., 2016. State of the art artificial intelligence-based MPPT techniques for mitigating partial shading effects on PV systems–A review. Renewable and Sustainable Energy Reviews, 64, pp.435-455.

[57] Islam, H., Mekhilef, S., Shah, N.B.M., Soon, T.K., Seyedmahmousian, M., Horan, B. and Stojcevski, A., 2018. Performance evaluation of maximum power point tracking approaches and photovoltaic systems. Energies, 11(2), p.365.

[58] Mohapatra, A., Nayak, B., Das, P. and Mohanty, K.B., 2017. A review on MPPT techniques of PV system under partial shading condition. Renewable and Sustainable Energy Reviews, 80, pp.854-867.

[59] Esram, T. and Chapman, P.L., 2007. Comparison of photovoltaic array maximum power point tracking techniques. IEEE Transactions on energy conversion, 22(2), pp.439-449.

[60] Pandey, A., Dasgupta, N. and Mukerjee, A.K., 2007. A simple single-sensor MPPT solution. IEEE Transactions on Power Electronics, 22(2), pp.698-700.

[61] Faranda, R., Leva, S. and Maugeri, V., 2008, July. MPPT techniques for PV systems: Energetic and cost comparison. In 2008 IEEE power and energy society general meeting-conversion and delivery of electrical energy in the 21st century (pp. 1-6). IEEE.

[62] Yu, G.J., Jung, Y.S., Choi, J.Y. and Kim, G.S., 2004. A novel two-mode MPPT control algorithm based on comparative study of existing algorithms. Solar Energy, 76(4), pp.455-463.

[63] Wang, H., Vinayagam, L., Jiang, H., Cai, Z.Q. and Li, H., 2016, September. New MPPT solar generation implemented with constant-voltage constant-current DC/DC converter. In 2016 51st International Universities Power Engineering Conference (UPEC) (pp. 1-6). IEEE.

[64] Lasheen, M., Abdel Rahman, A.K., Abdel-Salam, M. and Ookawara, S., 2017. Adaptive reference voltage-based MPPT technique for PV applications. IET Renewable Power Generation, 11(5), pp.715-722.

[65] Kota, V.R. and Bhukya, M.N., 2017. A novel linear tangents based P&O scheme for MPPT of a PV system. Renewable and Sustainable Energy Reviews, 71, pp.257-267.

[66] Sher, H.A., Murtaza, A.F., Noman, A., Addoweesh, K.E., Al-Haddad, K. and Chiaberge, M., 2015. A new sensorless hybrid MPPT algorithm based on fractional short-circuit current measurement and P&O MPPT. IEEE Transactions on sustainable energy, 6(4), pp.1426-1434.

[67] Frezzetti, A., Manfredi, S. and Suardi, A., 2014. Adaptive FOCV-based control scheme to improve the MPP tracking performance: an experimental validation. IFAC Proceedings Volumes, 47(3), pp.4967-4971.

[68] Ishaque, K. and Salam, Z., 2013. A review of maximum power point tracking techniques of PV system for uniform insolation and partial shading condition. Renewable and Sustainable Energy Reviews, 19, pp.475-488.

[69] Ahmed, A., Ran, L. and Bumby, J., 2012, May. Perturbation parameters design for hill climbing MPPT techniques. In 2012 IEEE International Symposium on Industrial Electronics (pp. 1819-1824). IEEE.

[70] Teulings, W.J.A., Marpinard, J.C., Capel, A. and O'sullivan, D., 1993, June. A new maximum power point tracking system. In Proceedings of IEEE Power Electronics Specialist Conference-PESC'93 (pp. 833-838). IEEE.

[71] Femia, N., Petrone, G., Spagnuolo, G. and Vitelli, M., 2005. Optimization of perturb and observe maximum power point tracking method. IEEE transactions on power electronics, 20(4), pp.963-973.

[72] Sera, D., Mathe, L., Kerekes, T., Spataru, S.V. and Teodorescu, R., 2013. On the perturb-and-observe and incremental conductance MPPT methods for PV systems. IEEE journal of photovoltaics, 3(3), pp.1070-1078.

[73] Pandey, A. and Srivastava, S., 2019. Perturb & observe MPPT technique used for PV system under different environmental conditions. Int. Res. J. Eng. Technol, 6(04), pp.2829-2835.

[74] Piegari, L. and Rizzo, R., 2010. Adaptive perturb and observe algorithm for photovoltaic maximum power point tracking. IET Renewable Power Generation, 4(4), pp.317-328.

[75] Alik, R. and Jusoh, A., 2017. Modified Perturb and Observe (P&O) with checking algorithm under various solar irradiation. Solar Energy, 148, pp.128-139.

[76] Manmohan, A., Prasad, A., Dharavath, R., Karthikeyan, S.P. and Raglend, I.J., 2017. Up and down conversion of photons with modified perturb and observe mppt technique for efficient solar energy generation. Energy Procedia, 117, pp.786-793.

[77] Zainuri, M.A.A.M., Radzi, M.A.M., Che Soh, A. and Rahim, N.A., 2014. Development of adaptive perturb and observe-fuzzy control maximum power point tracking for photovoltaic boost dc–dc converter. IET Renewable Power Generation, 8(2), pp.183-194.

[78] Jiang, Y., Qahouq, J.A.A. and Haskew, T.A., 2012. Adaptive step size with adaptive-perturbation-frequency digital MPPT controller for a single-sensor photovoltaic solar system. IEEE transactions on power Electronics, 28(7), pp.3195-3205.

[79] Kollimalla, S.K. and Mishra, M.K., 2014. A novel adaptive P&O MPPT algorithm considering sudden changes in the irradiance. IEEE Transactions on Energy conversion, 29(3), pp.602-610.

[80] Khaehintung, N., Wiangtong, T. and Sirisuk, P., 2006, October. FPGA implementation of MPPT using variable step-size P&O algorithm for PV applications. In 2006 international symposium on communications and information technologies (pp. 212-215). IEEE.

[81] Safari, A. and Mekhilef, S., 2010. Simulation and hardware implementation of incremental conductance MPPT with direct control method using cuk converter. IEEE transactions on industrial electronics, 58(4), pp.1154-1161.

[82] Hsieh, G.C., Hsieh, H.I., Tsai, C.Y. and Wang, C.H., 2012. Photovoltaic power-increment-aided incremental-conductance MPPT with two-phased tracking. IEEE Transactions on Power Electronics, 28(6), pp.2895-2911.

[83] Faraji, R., Rouholamini, A., Naji, H.R., Fadaeinedjad, R. and Chavoshian, M.R., 2014. FPGA-based real time incremental conductance maximum power point tracking controller for photovoltaic systems. IET Power Electronics, 7(5), pp.1294-1304.

[84] Kandemir, E., Cetin, N.S. and Borekci, S., 2017. A comprehensive overview of maximum power extraction methods for PV systems. Renewable and sustainable energy reviews, 78, pp.93-112.

[85] Desai, H.P. and Patel, H.K., 2007, November. Maximum power point algorithm in PV generation: An overview. In 2007 7th International Conference on Power Electronics and Drive Systems (pp. 624-630). IEEE.

[86] Salas, V., Olías, E., Barrado, A. and Lazaro, A., 2006. Review of the maximum power point tracking algorithms for stand-alone photovoltaic systems. Solar energy materials and solar cells, 90(11), pp.1555-1578.

[87] Huynh, D.C. and Dunnigan, M.W., 2016. Development and comparison of an improved incremental conductance algorithm for tracking the MPP of a solar PV panel. IEEE transactions on sustainable energy, 7(4), pp.1421-1429.

[88] Loukriz, A., Haddadi, M. and Messalti, S., 2016. Simulation and experimental design of a new advanced variable step size Incremental Conductance MPPT algorithm for PV systems. ISA transactions, 62, pp.30-38.

[89] Tey, K.S. and Mekhilef, S., 2014. Modified incremental conductance algorithm for photovoltaic system under partial shading conditions and load variation. IEEE Transactions on Industrial Electronics, 61(10), pp.5384-5392.

[90] Sivakumar, P., Kader, A.A., Kaliavaradhan, Y. and Arutchelvi, M., 2015. Analysis and enhancement of PV efficiency with incremental conductance MPPT technique under non-linear loading conditions. Renewable Energy, 81, pp.543-550.

[91] Reisi, A.R., Moradi, M.H. and Jamasb, S., 2013. Classification and comparison of maximum power point tracking techniques for photovoltaic system: A review. Renewable and sustainable energy reviews, 19, pp.433-443.

[92] Rajesh, R. and Mabel, M.C., 2014. Efficiency analysis of a multi-fuzzy logic controller for the determination of operating points in a PV system. Solar Energy, 99, pp.77-87.

[93] Choi, B.J., Kwak, S.W. and Kim, B.K., 2000. Design and stability analysis of single-input fuzzy logic controller. IEEE Transactions on Systems, Man, and Cybernetics, Part B (Cybernetics), 30(2), pp.303-309.

[94] Gupta, A.K. and Saxena, R., 2016, February. Review on widely-used MPPT techniques for PV applications. In 2016 international conference on innovation and challenges in cyber security (ICICCS-INBUSH) (pp. 270-273). IEEE.

[95] Syafaruddin, Karatepe, E. and Hiyama, T., 2009. Artificial neural network-polar coordinated fuzzy controller based maximum power point tracking control under partially shaded conditions. IET Renewable Power Generation, 3(2), pp.239-253.

[96] Priyadarshi, N., Azam, F., Sharma, A.K. and Vardia, M., 2019, July. An adaptive neuro-fuzzy inference system-based intelligent grid-connected photovoltaic power generation. In Advances in Computational Intelligence: Proceedings of Second International Conference on Computational Intelligence 2018 (pp. 3-14). Singapore: Springer Singapore.

[97] Kottas, T.L., Boutalis, Y.S. and Karlis, A.D., 2006. New maximum power point tracker for PV arrays using fuzzy controller in close cooperation with fuzzy cognitive networks. IEEE Transactions on Energy conversion, 21(3), pp.793-803.

[98] Bahgat, A.B.G., Helwa, N.H., Ahmad, G.E. and El Shenawy, E.T., 2005. Maximum power point traking controller for PV systems using neural networks. Renewable energy, 30(8), pp.1257-1268.

[99] Reatti, A. and Balzani, M., 2005. Neural network based model of a PV array for the optimum performance of PV system. In Proceedings of IEEE Research in Microelectronics and Electronics, 2005 (Vol. 2, pp. 123-126). IEEE.

[100] Mellit, A. and Pavan, A.M., 2010. A 24-h forecast of solar irradiance using artificial neural network: Application for performance prediction of a grid-connected PV plant at Trieste, Italy. Solar energy, 84(5), pp.807-821.

[101] Giraud, F. and Salameh, Z.M., 2002. Analysis of the effects of a passing cloud on a grid-interactive photovoltaic system with battery storage using neural networks. IEEE Transactions on Energy Conversion, 14(4), pp.1572-1577.

[102] Ramana, V.V. and Jena, D., 2015, February. Maximum power point tracking of PV array under non-uniform irradiance using artificial neural network. In 2015 IEEE International Conference on Signal Processing, Informatics, Communication and Energy Systems (SPICES) (pp. 1-5). IEEE.

[103] Hiyama, T., Kouzuma, S. and Imakubo, T., 2002. Identification of optimal operating point of PV modules using neural network for real time maximum power tracking control. IEEE Transactions on Energy Conversion, 10(2), pp.360-367.

[104] M. A. Younis, T. Khatib, M. Najeeb, and A. M. Ariffin, "An improved maximum power point tracking controller for PV systems using artificial neural network," Przegla¸d Elektrotechniczny (Electrical Review), vol. 88, no. 3b, pp. 116–121, Jan. 2012.

[105] Rai, A.K., Kaushika, N.D., Singh, B. and Agarwal, N., 2011. Simulation model of ANN based maximum power point tracking controller for solar PV system. Solar Energy Materials and Solar Cells, 95(2), pp.773-778.

[106] Kulaksız, A.A. and Akkaya, R., 2012. A genetic algorithm optimized ANN-based MPPT algorithm for a stand-alone PV system with induction motor drive. Solar Energy, 86(9), pp.2366-2375.

[107] Kato, H. and Yamauchi, K., 2015, October. Quick MPPT microconverter using a limited general regression neural network with adaptive forgetting. In 2015 International Conference on Sustainable Energy Engineering and Application (ICSEEA) (pp. 42-48). IEEE.

[108] Elobaid, L.M., Abdelsalam, A.K. and Zakzouk, E.E., 2012, October. Artificial neural network based maximum power point tracking technique for PV systems. In IECON 2012-38th Annual Conference on IEEE Industrial Electronics Society (pp. 937-942). IEEE.

[109] Liu, Y.H., Chen, J.H. and Huang, J.W., 2015. A review of maximum power point tracking techniques for use in partially shaded conditions. Renewable and Sustainable Energy Reviews, 41, pp.436-453.

[110] Cabal, C., Martínez-Salamero, L., Séguier, L., Alonso, C. and Guinjoan, F., 2014. Maximum power point tracking based on sliding-mode control for output-series connected converters in photovoltaic systems. IET Power Electronics, 7(4), pp.914-923.

[111] Tan, S.C., Lai, Y.M. and Chi, K.T., 2008. General design issues of sliding-mode controllers in DC–DC converters. IEEE transactions on industrial electronics, 55(3), pp.1160-1174.

[112] Montoya, D.G., Ramos-Paja, C.A. and Giral, R., 2015. Improved design of sliding-mode controllers based on the requirements of MPPT techniques. IEEE transactions on Power Electronics, 31(1), pp.235-247.

[113] Kim, I.S., Kim, M.B. and Youn, M.J., 2006. New maximum power point tracker using sliding-mode observer for estimation of solar array current in the grid-connected photovoltaic system. IEEE Transactions on industrial Electronics, 53(4), pp.1027-1035.

[114] Zhang, M., Wu, J. and Zhao, H., 2004, June. The application of slide technology in PV maximum power point tracking system. In Fifth world congress on intelligent control and automation (IEEE Cat. No. 04EX788) (Vol. 6, pp. 5591-5594). IEEE.

[115] Bianconi, E., Calvente, J., Giral, R., Mamarelis, E., Petrone, G., Ramos-Paja, C.A., Spagnuolo, G. and Vitelli, M., 2013. Perturb and observe MPPT algorithm with a current controller based on the sliding mode. International Journal of Electrical Power & Energy Systems, 44(1), pp.346-356.

[116] Bianconi, E., Calvente, J., Giral, R., Mamarelis, E., Petrone, G., Ramos-Paja, C.A., Spagnuolo, G. and Vitelli, M., 2012. A fast current-based MPPT technique employing sliding mode control. IEEE Transactions on Industrial Electronics, 60(3), pp.1168-1178.

[117] Yu, M.Q., 2018, July. Parameter identification of photovoltaic cell model based on perturbation and observation and modified Gauss-Newton method. In 2018 37th Chinese Control Conference (CCC) (pp. 6127-6131). IEEE.

[118] Xiao, W., Dunford, W.G., Palmer, P.R. and Capel, A., 2007. Application of centered differentiation and steepest descent to maximum power point tracking. IEEE Transactions on Industrial Electronics, 54(5), pp.2539-2549.

[119] Hu, Y. and Fang, L., 2019. Two modifications of efficient newton-type iterative method and two variants of Super-Halley's method for solving nonlinear equations. Journal of Computational Methods in Science and Engineering, 19(1), pp.13-22.

[120] Farayola, A.M., Hasan, A.N. and Ali, A., 2018. Efficient photovoltaic mppt system using coarse gaussian support vector machine and artificial neural network techniques. International Journal of Innovative Computing Information and Control (IJICIC), 14(1), pp.323-329.

[121] Enslin, J.H., Wolf, M.S., Snyman, D.B. and Swiegers, W., 2002. Integrated photovoltaic maximum power point tracking converter. IEEE Transactions on industrial electronics, 44(6), pp.769-773.

[122] Jabbar, R.I., Mekhilef, S., Mubin, M. and Mohammed, K.K., 2023. A modified perturb and observe MPPT for a fast and accurate tracking of MPP under varying weather conditions. IEEE Access, 11, pp.76166-76176.

[123] Abouzeid, A.F., Eleraky, H., Kalas, A., Rizk, R., Elsakka, M.M. and Refaat, A., 2024. Experimental validation of a low-cost maximum power point tracking technique based on artificial neural network for photovoltaic systems. Scientific Reports, 14(1), p.18280.

[124] Dang, V.T., Yang, M.G., Shim, Y., Lee, W. and Baek, K.H., 2021. An accurate time-based MPPT circuit with two-period tracking algorithm and convergence range averaging technique for IoT applications. IEEE Access, 9, pp.31401-31410.

[125] Mei, Q., Shan, M., Liu, L. and Guerrero, J.M., 2010. A novel improved variable step-size incremental-resistance MPPT method for PV systems. IEEE transactions on industrial electronics, 58(6), pp.2427-2434.

[126] Ali, Z.M., Alquthami, T., Alkhalaf, S., Norouzi, H., Dadfar, S. and Suzuki, K., 2022. Novel hybrid improved bat algorithm and fuzzy system based MPPT for photovoltaic under variable atmospheric conditions. Sustainable Energy Technologies and Assessments, 52, p.102156.

[127] González-Castaño, C., Restrepo, C., Kouro, S. and Rodriguez, J., 2021. MPPT algorithm based on artificial bee colony for PV system. Ieee Access, 9, pp.43121-43133.

[128] Tao, H., Ghahremani, M., Ahmed, F.W., Jing, W., Nazir, M.S. and Ohshima, K., 2021. A novel MPPT controller in PV systems with hybrid whale optimization-PS algorithm based ANFIS under different conditions. Control Engineering Practice, 112, p.104809.

[129] Aguila-Leon, J., Vargas-Salgado, C., Chiñas-Palacios, C. and Díaz-Bello, D., 2023. Solar photovoltaic Maximum Power Point Tracking controller optimization using Grey Wolf Optimizer:

A performance comparison between bio-inspired and traditional algorithms. Expert Systems with Applications, 211, p.118700.

[130] Manna, S., Akella, A.K. and Singh, D.K., 2023. Implementation of a novel robust model reference adaptive controller-based MPPT for stand-alone and grid-connected photovoltaic system. Energy Sources, Part A: Recovery, Utilization, and Environmental Effects, 45(1), pp.1321-1345.

Appendix A

Code for Modified P&O Algorithm

<u>Modified P&O method:</u>

```
function duty = enhanced_po_zones(vpv, ipv)

% Parameters
duty_init = 0.1;
duty_min = 0;
duty_max = 0.85;

% Estimated Vmpp of your panel
Vmpp_est = 301;
V1 = 0.9 * Vmpp_est;  % Left boundary
V2 = 1.1 * Vmpp_est;  % Right boundary

% Step sizes
delta_large = 200e-6;
delta_small = 20e-6;

% MPP slope threshold
epsilon = 0.05;

% Persistent variables
persistent Vprev Pprev duty_old

if isempty(Vprev)
    Vprev = 0;
    Pprev = 0;
    duty_old = duty_init;
end

% Power and differences
P = vpv * ipv;
dV = vpv - Vprev;
dP = P - Pprev;

% Derivative
if abs(dV) > 1e-6
    dPdV = dP / dV;
```

```
else
    dPdV = 0;
end

% Select delta based on VPV zone
if vpv < V1 || vpv > V2
    delta = delta_large;  % Far from MPP ? bigger step
else
    delta = delta_small;  % Near MPP ? smaller step
end

% Apply P&O logic with slope and zone awareness
if abs(dPdV) > epsilon && vpv > 30
    if dPdV > 0
        duty = duty_old - delta;  % Move left
    else
        duty = duty_old + delta;  % Move right
    end
else
    duty = duty_old;  % In MPP region
end

% Clamp duty cycle
duty = max(min(duty, duty_max), duty_min);

% Update memory
Vprev = vpv;
Pprev = P;
duty_old = duty;

end
```

Appendix B

Code for P&O Algorithm

P&O method:

```
function duty = po(vpv, ipv, delta)

duty_init = 0.1;
duty_min = 0;
duty_max =0.85;

persistent Vold Pold duty_old;

if isempty(Vold)
    Vold = 0;
    Pold = 0;
    duty_old = duty_init;
end
P = vpv*ipv;
dV = vpv - Vold;
dP =P - Pold;

if dP ~= 0 && vpv>30
    if dP<0
        if dV<0
            duty = duty_old - delta;
        else
            duty = duty_old + delta;
        end
    else
        if dV<0
            duty = duty_old + delta;
        else
            duty = duty_old - delta;
        end
    end
else
   duty = duty_old;
end
```

```
if duty >= duty_max
    duty = duty_max;
elseif duty<duty_min
    duty = duty_min;
end

duty_old = duty;
Vold = vpv;
Pold = P;
```

Appendix C

Code for Incremental Conductance Algorithm

Incremental Conductance Method:

```
function duty = inc_cond(vpv, ipv, delta)

duty_init = 0.1;
duty_min = 0;
duty_max = 0.85;

persistent Vold Iold duty_old;

if isempty(Vold)
    Vold = 0;
    Iold = 0;
    duty_old = duty_init;
end

% Current slope values
dV = vpv - Vold;
dI = ipv - Iold;

if vpv > 30   % avoid startup oscillations at very low
voltage

    if dV == 0
        if dI == 0
            % At MPP ? duty unchanged
            duty = duty_old;
        elseif dI > 0
            % Left of MPP ? decrease duty (raise V)
            duty = duty_old - delta;
        else
            % Right of MPP ? increase duty (lower V)
            duty = duty_old + delta;
        end
    else
        if (dI/dV) == -(ipv/vpv)
            % At MPP
            duty = duty_old;
        elseif (dI/dV) > -(ipv/vpv)
```

```
            % Left of MPP ? decrease duty (raise V)
            duty = duty_old - delta;
        else
            % Right of MPP ? increase duty (lower V)
            duty = duty_old + delta;
        end
    end

else
    duty = duty_old;
end

% Limit duty cycle
if duty >= duty_max
    duty = duty_max;
elseif duty < duty_min
    duty = duty_min;
end

% Update persistent values
duty_old = duty;
Vold = vpv;
Iold = ipv;

end
```

Appendix D

Simulink connection diagram of proposed system

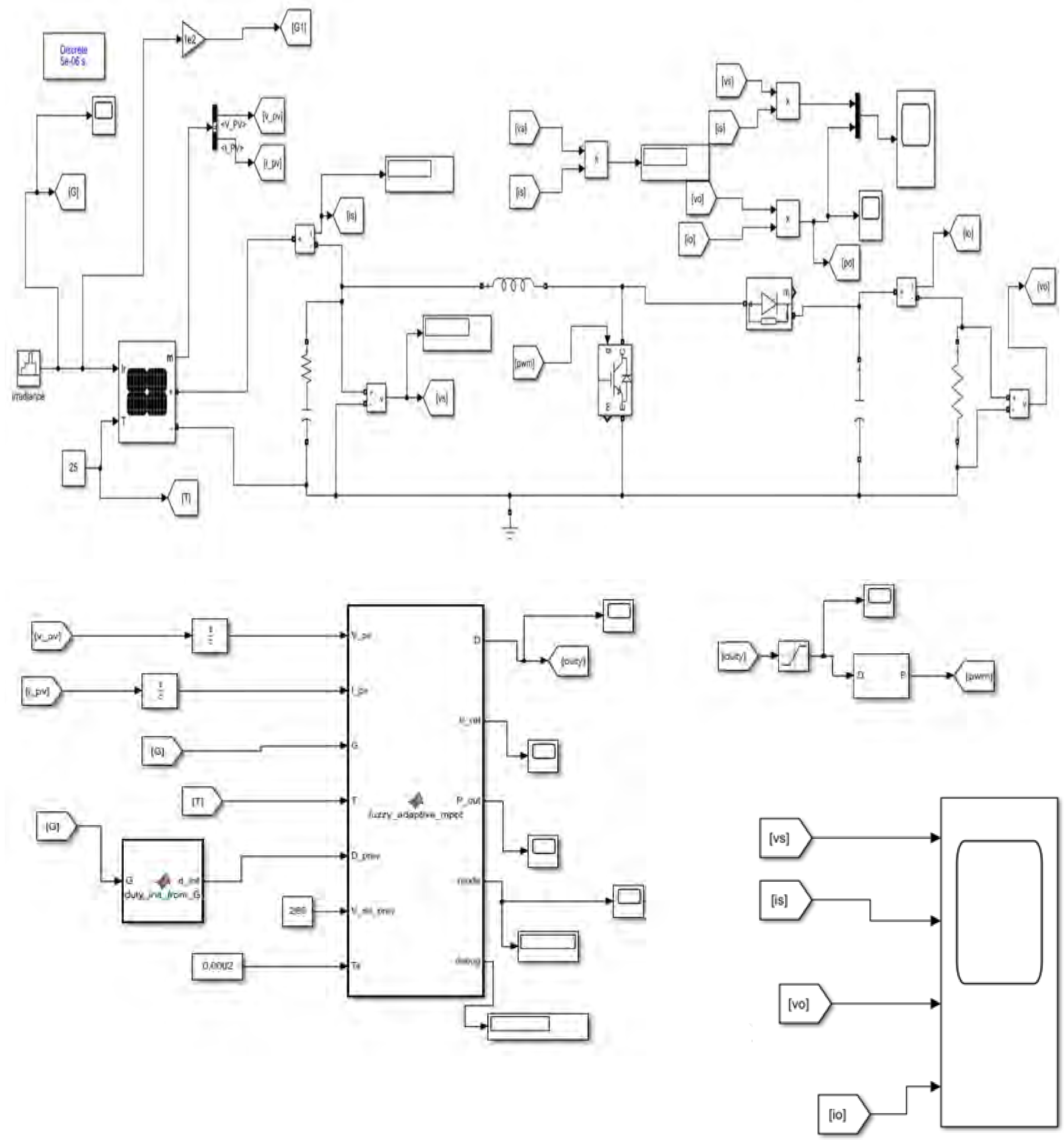

Appendix E

Current and Voltage waveforms of proposed system

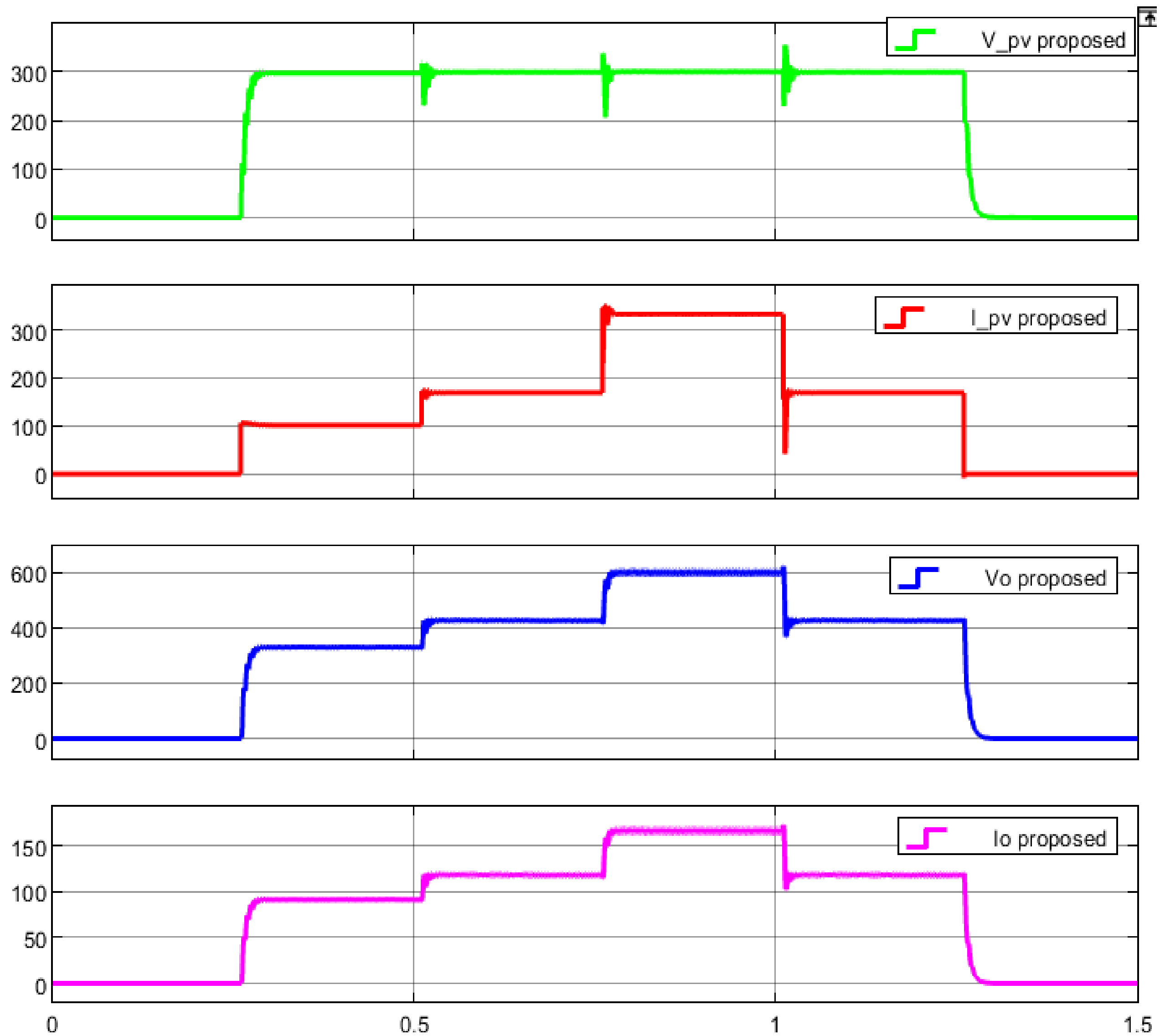

Appendix F

Input and Output Power curves of proposed system